RIGA TECHNICAL UNIVERSITY

Guntis Spriņģis

ANALYSIS AND CALCULATION OF WEAR FOR SLIDING FRICTION PAIR

Summary of the Doctoral Thesis

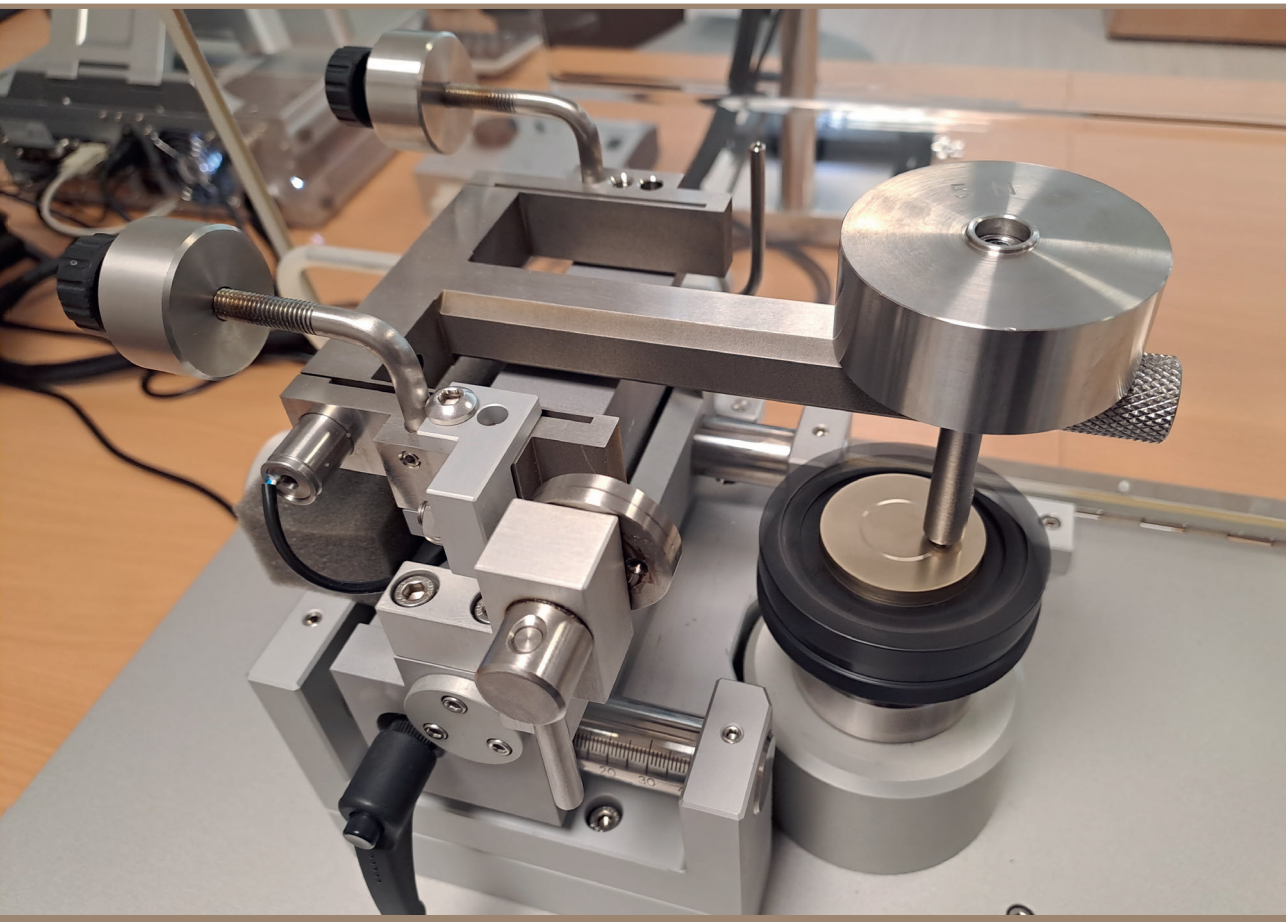

RTU Press
Riga 2023

RIGA TECHNICAL UNIVERSITY
Faculty of Mechanical Engineering, Transport and Aeronautics
Institute of Mechanics and Mechanical Engineering

Guntis Spriņģis
Doctoral Student of the Study Programme "Mechanical Engineering and Mechanics"

ANALYSIS AND CALCULATION OF WEAR FOR SLIDING FRICTION PAIR

Summary of the Doctoral Thesis

Scientific supervisors

Professor Dr. sc. ing.
IRĪNA BOIKO

Professor Dr. habil. sc. ing.
JĀNIS RUDZĪTIS

RTU Press
Riga 2023

Spriņģis, G. Analysis and Calculation of Wear for Sliding Friction Pair. Summary of the Doctoral Thesis. – Riga: RTU Press, 2023. – 57 p.

Published in accordance with the decision of the Promotion Council "RTU P-04" of 28 November 2023, Minutes No. 58.

The Thesis was developed with the support from the European Social Fund within the framework of the Specific Support Objective 8.2.2 of the Operational Programme "Growth and Employment" "Strengthening the academic staff of higher education institutions in areas of strategic specialisation" Project No. 8.2.2.0/20/I/008 "Strengthening the doctoral students and academic staff of Riga Technical University and Banking University in areas of strategic specialisation".

Cover picture by Guntis Spriņģis

https://doi.org/10.7250/9789934370212
ISBN 978-9934-37-021-2 (pdf)

DOCTORAL THESIS PROPOSED TO RIGA TECHNICAL UNIVERSITY FOR THE PROMOTION TO THE SCIENTIFIC DEGREE OF DOCTOR OF SCIENCE

To be granted the scientific degree of Doctor of Science (Ph. D.), the present Doctoral Thesis has been submitted for the defence at the open meeting of RTU Promotion Council on December 29, 2023, at the Faculty of Riga Technical University, 6B Ķīpsalas Street, Room 521.

OFFICIAL REVIEWERS

Professor Dr. sc. ing. Igors Tipāns,
Riga Technical University

Senior Researcher, PhD Maksim Antonov,
Tallinn University of Technology, Estonia

Associate Professor DSc, PhD Dariusz Mariusz Perkowski
Bialystok University of Technology, Poland

DECLARATION OF ACADEMIC INTEGRITY

I hereby declare that the Doctoral Thesis submitted for review to Riga Technical University for promotion to the scientific degree of Doctor of Science (Ph. D.) is my own. I confirm that this Doctoral Thesis has not been submitted to any other university for promotion to a scientific degree.

Guntis Spriņģis ……. (signature)

Date: ……

The Doctoral Thesis has been written in Latvian. It consists of an Introduction, 5 chapters, Conclusions, 64 figures, 18 tables, and 2 appendices; the total number of pages is 95, not including appendices. The bibliography contains 93 titles.

TABLE OF CONTENTS

GENERAL CHARACTERISTICS OF THE THESIS

Actuality of the topic

Today, the manufacturing process of components in engineering and other industries uses the latest technologies and new material combinations to extend products' lifetime. The development of a sustainable economy is inconceivable without a shift towards resource efficiency, which can also be achieved by increasing the lifetime of products: the safe and durable use of products will allow more efficient and rational management of natural and productive resources and will also directly contribute to other sustainability-related objectives, such as ensuring a safe environment, reducing pollution and reducing the consumption of energy and other resources.

To prolong the service life of products containing friction couples and to renew surfaces worn by friction couples in service, not only traditional and long-established but also modern technologies are now used, such as surface treatment and hardening by laser and electron beam treatment, various types of surface heating methods, ion-plasma vacuum treatment, etc. [43], [44]. In addition to solutions to improve the performance of component surfaces, it is also necessary to predict the lifetime of these components to optimise the production process and make the necessary adjustments to the manufacturing process in good time. One of the main criteria for determining the future operation of components is wear. Although several techniques and computational methods are currently available to determine wear analytically, predicting wear based on lengthy, time-consuming and costly experiments is still prevalent. This is because the analytical wear calculation would need to describe parameters present in the actual wear process, which, in most cases, is not done because of the wear process complexity.

To calculate wear values more precisely, it is necessary to describe the contact and wear process between the two friction surfaces and to include prevailing friction process parameters that are easy to determine and reflect the actual wear process as accurately as possible.

An analytical prediction of the service life of friction pairs is valid for practical engineering tasks and includes standardised parameters that modern measurement methods can determine without the need for lengthy and resource-intensive experiments. It not only speeds up the product design process but also makes a significant contribution to sustainable development.

Therefore, the Thesis topic is relevant for both science and economy, as it is related to eliminating certain shortcomings in the methodologies for predicting the service life of a friction pair, which will significantly impact the efficiency of research and design.

Hypothesis: The introduction of surface texture (3D) parameters, as well as the refinement of individual material fatigue parameter's values in the sliding friction pair wear calculation, will increase the accuracy of the calculation by synthesising a new

mathematical model for the wear calculation and developing a methodology for predicting the lifetime of the friction pair.

Aim and objectives of the Thesis

The Thesis aims to synthesise a new mathematical model for the wear calculation of friction pairs and to develop a methodology for predicting the lifetime of a friction pair.

To achieve the objectives, the following tasks were defined:

1. Search and analyse information sources.
2. Carry out pilot experimental studies.
3. Develop a friction surface contact model that incorporates the friction surface's texture (3D) parameters.
4. Synthesise a new mathematical model for calculating the friction pair's wear.
5. Develop a new methodology for predicting the lifetime of a friction pair.
6. Validate the new wear prediction methodology for the friction pair.

Research methods

Quantitative and qualitative research methods, as well as technical support for the experiments listed below, were used to achieve the defined objective and solve the tasks.

The theoretical calculations were based on elasticity theory, surface contact theory, surface material's fatigue theory, a separate section of probability theory (random field), and normal distribution law.

A *Mitutoyo FORMTRACER Avant 3D* (*Mitutoyo*, Japan) was used to measure the required surface texture (3D) parameters. A *Mitutoyo SURFTEST SJ-500* roughness profilometer (*Mitutoyo*, Japan) and a *Taylor Hobson SURTRONIC 25* portable profilometer (*Taylor Hobson*, UK) were used to measure the surface roughness parameters and to determine the worn track parameters. The diameter of the ball's flat area was measured before and after the experiment using a *Hirox* digital microscope (*Hirox*, Japan).

The experiments used a *CSM* tribometer (*CSM Tribometer*, Switzerland) and a self-built friction and wear test machine in combination with a *PCE FG-50* electronic dynamometer (*PCE Instruments UK Ltd*, UK) and revolution counter *ALLURIS SMF-50* (*Alluris*, Germany) for the sliding friction pair. In the first stage of the experimental studies, the length of the pressure roller was controlled using a *Mitutoyo* digital micrometer (*Mitutoyo*, Japan) with an accuracy of 0.001 mm.

InstrumX software (*CSM Instruments*, Switzerland) was used to record, process and analyse the experimental data (friction coefficient, wear time/distance, etc.). *TalyMap Gold* (*Taylor Hobson*, UK), *MCube Map Ultimate 8*, *Microsoft Excel*, and *MathCad* software were used to process and analyse the experimental data. The results are presented in the form of graphs, figures and tables.

Scientific novelty

1. A new contact model for friction surfaces that incorporates (3D) friction surface texture parameters.
2. A new mathematical model for wear calculation, synthesised on the basis of a new friction surface model and considering material deformation parameters.
3. A new wear prediction methodology to determine a friction pair's lifetime and analyse and synthesise the optimum parameter values for maximum lifetime.

Theses to be defended

1. A new analytical model for predicting friction pair wear is synthesised based on a developed friction surface contact model, which incorporates friction surface texture (3D) parameters, providing a more complete surface description, which is essential for wear calculation and provides a more accurate calculation compared to previously known analytical models.
2. A new methodology for predicting the lifetime of a sliding friction pair provides a more accurate prediction than previously known methodologies.
3. Experimental results that validate the applicability of the developed analytical model for friction pair wear prediction and the methodology for predicting the life of a sliding friction pair for engineering calculations.

Practical significance of the Thesis

The results of the Thesis can be used in research and industry. In the study of wear, it is recommended to use the friction surface contact model, the wear calculation model and the wear prediction methodology for friction pairs developed in the framework of the Thesis because, for the first time, the models and methodologies integrate texture (3D) parameters, which (as shown by several known studies [35]–[37], [39], [40], [42] describe the surfaces of the parts more completely and accurately, while the wear calculation model includes deformation mode and stress parameters. The results of the Thesis show that this approach provides a more accurate prediction of the lifetime of a friction pair compared to previously known approaches and, compared to previously known wear calculation methodologies, the methodology developed in the Thesis includes easily identifiable standardised characteristics and material properties.

Furthermore, the new friction pair wear prediction methodology developed in the Thesis allows the lifetime of friction pairs to be predicted analytically, eliminating the need for time-consuming and labour-intensive experiments, which is relevant in research and industry. The methodology has been used in the work of Naco Ltd within the contract project No. 1/22.05.2013-3, “Investigation of the methodology for the calculation of wear of nanostructured coatings using the plasticity and elasticity characteristics of the coating”.

The results of the Thesis have also been recognised as important by the Association of Mechanical Engineering and Metalworking Industry (MASOC), and the newly developed wear calculation methodology has been published on the MASOC website (in the section available to MASOC members) and is thus available to more than 160 Latvian companies in the relevant industry – MASOC members. The main results of the Thesis have also been validated at several international scientific conferences and published in scientific journals.

Approbation of obtained results

International scientific conferences (the most important ones are listed)

1. Springis, G., Boiko, I. Studies of experimental results and analytical calculations of wear of friction pair "steel-anti-friction material". 64th International Scientific Conference of Riga Technical University *Mechanical engineering technology and heat engineering*, 12 October 2023, Riga, Latvia. **With published abstract.**
2. Springis, G., Boiko, I. Comparison of Experimental and Theoretical Wear Studies of Sliding Friction Pairs of Metallic Surfaces. Riga Technical University 61st International Scientific Conference *Mechanical Engineering Technology and Heat Engineering*, 14 October 2020, Riga, Latvia. **With published abstract.**
3. Springis, G., Rudzitis, J., Gerins, E., Bulaha, N. Theoretical Approach of Wear for Slide-Friction Pairs. 12th International Conference *Mechatronic Systems and Materials Intelligent Technical Systems*, July 3–8, 2016. Bialystok, Poland. **With published abstract.**
4. Springis, G., Rudzitis, J., Avisane, A., Kumermanis, M., Semjonovs, J., Leitans, A. Wear problems of slide-friction pairs. The 9th International Conference *Mechatronic Systems and Materials* (MSM 2013), July 1–3, 2013, Vilnius, Lithuania. **With published abstract.**
5. Springis, G., Rudzitis, J., Avisane, A., Kumermanis, M. Wear Calculation Possibility of Slide-Friction Pair 'Shaft-Plain Bearing' for Four-Stroke Engines". 3rd International Advances in Applied Physics & Materials Science Congress. Antalya, Turkey, AIP Conference Proceedings, 24–28 April 2013. **With published abstract.**
6. Springis, G., Rudzitis, J. Wear calculation models for slide friction pairs, Riga Technical University 53rd International Scientific Conference dedicated to the 150th anniversary and the 1st Congress of World Engineers and Riga Polytechnical Institute/RTU Alumni, 11–12 October 2012, Riga, Latvia. **With published abstract.**

Publications in scientific journals (indexed in SCOPUS)

1. Springis, G., Boiko, I., Linins, O. Calculation of Wear of Metallic Surfaces Using Material's Fatigue Model and 3D Texture Parameters. *Tribology in Industry,* Vol. 45, 2023, pages 729-741. Pieejams: doi: 10.24874/ti.1581.11.23.12.
2. Springis, G., Rudzitis, J., Avisane, A., Leitans, A. Wear Calculation for Sliding Friction Pairs. *Latvian Journal of Physics and Technical Sciences*, Vol. 2, 2014, pages 41–54. ISSN 2255-8896. Available: doi: 10.2478/lpts-2014-0012.

Full-text conference proceedings/journal articles (indexed in SCOPUS)

1. Springis, G., Boiko, I., Kononova, O. Optimisation of the parameters included in the wear analysis model to increase the service life of the friction pair. 23rd International

Scientific Conference *Engineering for Rural Development*: Proceedings. Latvia, Jelgava, 22–24 May 2024, 6 pages. (*Submitted*).
2. Springis, G., Rudzitis, J., Lungevics, J., Berzins, K. Wear Calculation Approach for Sliding-Friction Pairs. Journal of Physics. Series 843 (2017) 012072. 2017, pages 1–8. ISSN 1742-6588. Available: doi: 10.1088/1742-6596/843/1/012072.
3. Springis, G., Rudzitis, J., Gerins, E., Bulaha, N. Theoretical Approach of Wear for Slide-Friction Pairs. Trans Tech Publications, 2017, pages 202–211. ISSN 1662-9779. Available: doi: https://doi.org/10.4028/www.scientific.net/SSP.260.202.
4. Springis, G., Rudzitis, J., Gerins, E., Leitans, A. Rough Surface Peak Influence on the Wear Process of Sliding-Friction Pairs. 15th International Scientific Conference *Engineering for Rural Development*: Proceedings. Vol. 15, Latvia, Jelgava, 25–27 May 2016, pages 1430–1436. ISSN 1691-3043. Available: http://www.tf.llu.lv/conference/proceedings2016/Papers/N283.pdf.
5. Springis, G., Rudzitis, J., Avisane, A., Kumermanis, M., Semjonovs, J., Leitans, A. Wear Problems of Slide-Friction Pair. Trans Tech Publications, Switzerland, *Solid State Phenomena*, Vol. (220–221), 2015, pages 361–366. ISSN 1662-9779. Available: doi: https://doi.org/10.4028/www.scientific.net/SSP.220-221.361.
6. Linins, O., Leitans, A., Springis, G., Rudzitis, J. Determining the Number of Peaks of Rough Surfaces Necessary for Wear Calculation, Trans Tech Publications, Switzerland, *Key Engineering Materials*, Vol. 604, 2014, pages 59–62. ISSN 1013-9826. Available: doi: https://doi.org/10.4028/www.scientific.net/KEM.604.59.

GLOSSARY

Sq – root mean square deviation from the midplane;
Sa – arithmetic mean deviation from the midplane;
RSm_1 – step perpendicular to the machining direction;
RSm_2 – a step towards processing;
Str – surface anisotropy coefficient;
V_Σ – volume of deformed surface asperities over the entire friction surface;
N_{cf} – the actual number of cycles to which the surface asperities are subjected during the friction process;
N_c – number of cycles leading to the destruction of the surface asperities;
L_b – friction path length;
RSm_2^a – the average surface roughness step of the surface contributing to the wearing of the other surface;
N_0 – number of cycles of resistance of the material under asymmetric loading;
t_σ – dimensionless stress ratio;
m – the degree of the material fatigue curve equation;
σ_0 – limit of durability of the material;
σ_a – stress amplitude;
$K(e)$ – 1st order elliptic integral;
μ – Poisson's ratio;
h_0 – the height of the paraboloid segment measured from the apex (thickness of the particle removed);
K_i – curvature of the i-th ridge of the roughness;
$h_{izc.}$ – height of the asperity,
u – deformation level;
$h_{atd.}$ – thickness of the particle separated during wear;
γ – relative height of the slit normalised by Sq;
k_q – coefficient depending on the surface anisotropy parameter Str;
E – modulus of elasticity of the material of the worn part;
q – load;
V_i – mean value of the volume separated by the i-th asperity;
N_γ – number of deformed asperities due to friction;
Sds – number of asperities on the rough surface.

1. LITERATURE REVIEW

This chapter reviews the literature on the most popular methods available for the analytical calculation and experimental determination of wear.

1.1. Theoretical and experimental approaches to wear calculations

Wear calculation approaches based on the Archard equation

Several wear calculation models have been developed over time to predict the lifetime of a joint. However, wear processes are influenced by various parameters such as surface geometry, physical-mechanical conditions, material of the parts, wear temperature, wear regime, etc. It is impossible to consider all these factors analytically. Therefore, wear calculations are developed based on multiple theories that take into account the complex of influencing variables.

A widely accepted method for calculating wear was devised by British scientist John F. Archard. This model is predicated on the notion that the most critical factors influencing wear are the load (F), material hardness (H), and sliding distance (l). The wear coefficient k should be known in advance:

$$W = k \cdot \frac{F \cdot l}{H}. \tag{1.1}$$

A review of the literature [1]–[3], [5]–[7], [10], [12], [26]–[28], [30], [33], [40] has indicated that Eq. (1.1), possibly adjusted to the specific surface geometry, materials, and wear conditions, is still commonly used. Wujiao et al. [1] studied the wear mechanism of hot forging dies and, by refining Eq. (1.1), proposed a wear calculation relationship that enables the prediction of die wear and the optimization of die geometry to extend die life. Adrian et al. [2] predicted the dry sliding wear of an automotive turbocharger shaft and bushing using the method developed by Archard, while Reichert et al. [3] evaluated the wear resistance of different shaft bearing materials in combination with a steel shaft, using the Archard's equation. Wan-Gi Cha et al. [5] modelled the wear of tool blades used in the dry cutting/sawing process of sheet metal by coupling the wear estimation Eq. (1.1) with the REDSY wear simulation tool to determine the changes in tool geometry caused by wear. Gao Deli et al. [6] used a calculation model based on Eq. (1.1) with modifications to investigate the depth of wear grooves inside the casing of a downhole attachment. Brandao et al. [7] performed a numerical simulation of the gear tooth surface wear based on a mixed lubrication model that considers the surface profile roughness parameters (Rz, Ra, and Rq), the lubricant properties, and a modified wear model of Eq. (1.1). Frischmuth et al. [10] integrated Archard's model into mathematical relationships according to the operating conditions of a high-speed train wheel to model wear. Dirks and Enblom [27] followed Archard's wear calculation equation, extended by Jendel, in which the contact patch is divided into cell elements of a certain size to determine the depth of wear for each cell. The purpose of the study is to establish a link between the wear model and the contact depth

model. Khader et. al. [26] examined the wear of rollers with silicon nitride surfaces using Archard's uniformity adapted to a specific calculation. Yuanpei Chen et. al. [28] used the wear calculation Eq. (1.1) modified by McColl et. al. to predict the wear of steel wires and integrated it into a mathematical model that also included additional parameters such as wire contact pressure, strain and internal stresses. Mukherjee et. al. [12] applied Eq. (1.1) in a simplified way to study the wear behaviour of SiC coatings, while Weijun Tao et al. [30] studied the wear of linear roller guides, which is directly related to the load applied to the guides. Popov et al. [31], [32] reviewed the possibilities of modifying Archard's equation, considering the theory developed by scientist E. Rabinovich on the formation of particles separated due to wear, considering the elastic modulus and hardness of the material and the work consumed during particle separation. The study aims to propose a formula for calculating wear by combining the theories developed by the two scientists mentioned above and carrying out a numerical simulation of the resulting relationships. Yanfei Liu et al. [40] investigated changes in the mechanical properties of a material due to friction by modifying Archard's classical wear calculation model. The author points out that when the surfaces of two parts are subjected to small amplitude oscillatory motions, significant changes in the mechanical properties and microstructure occur on the surface of the material, but Archard's original model did not take these factors into account.

Mixed wear calculation models

In their study, Fei Lyu etal [8] focus on the wear between the piston and cylinder of an axial pump and propose wear prediction equations based on the relationship between bearing loading and lubrication parameters. It is important to note that the friction coefficient included in their wear calculation model is determined experimentally and does not have any predefined theoretical justification or limits assumed in the calculation formula. This can significantly affect the accuracy of the calculation results. Kloss et al. [11] consider two methods, the mass balance and the energy balance wear calculation method. Sakurai et al. [11] also use a similar approach to describe the formation of iron sulphide layers in a lubricated tribosystem using radioactive sulphur and sulphur compounds. Dorinson and Ludem describe the metal transfer and oxidation during wear, while Fillot et al. use this concept to model the wear behaviour of granular materials during the wear process [11].

Determination of the wear values by experimental studies

Many researchers use experimental methods to determine wear values instead of analytical calculations. For instance, Wenfang Cui et al. [19] analysed the properties of nano-TiN coatings on Ti alloys by measuring the parameters of the worn track using a sphere-disk-type tribometer to determine the wear rate. Sajjad Ghasemi et al. [20] also used this type of tribometer to study Ti/TiN coatings on Al 7075 substrate by measuring the width and depth of the worn track. Similarly, Lari Baghal et al. [21] evaluated the wear of Ni-Co/SiC coatings on Al substrate by determining the wear rate and weighing

the mass of material removed. Xu Bin-shi et al. [18] measured the depth of the worn track left by the bullet to determine the amount of wear in experimental studies on a coated surface. Vatan et al. [22] tested the tribological properties of WC nanocomposite coatings on Mg alloys by both weighing the samples and measuring the geometrical parameters of the worn track left by the ball to evaluate wear. Bahshwan et al. [25] conducted experiments to determine the wear rate experimentally while studying the wear properties of steel parts produced using additive manufacturing technology. In their work, Kiranagi et al. [24] discussed the units of measurement used by scientists to analyse the wear values obtained by experiments. Dehgagi et al. [13] carried out wear tests to analyse the corrosion and wear properties of Ni-Al O23 -SiC coatings, and the processing of the measured data led to the conclusion of the predominant type of wear and the intensity of wear. Lin Ding et al. [14] analysed the effect of nano-CeO2 on the microstructure and wear resistance of Co-based coatings, the numerical values of the weight wear (in milligrams), one of the most important output parameters, were only obtained by experiments. Yazdani et al. [16] investigated the properties of nanostructured functionally graded Ni-Al O23 composite coatings and also used experimentally obtained wear rates. Walker et al. [17] analysed Fe nanoparticle coatings designed to increase wear resistance at high temperatures and used two methods to determine wear, either by weighing or by reconstructing the original geometric shape of the part so that the amount of material worn can be calculated as a result. Vereschaka et al. [23] analysed the parameters of cutting inserts with different types of coatings ((Ti, Al))CN and Ti-TiCN-(Ti, Al, Cr)CN in the steel machining process and paid special attention to the determination of wear by measuring the relevant parameters of the worn insert with an instrumental microscope.

Wear calculation model by Pronikov et al.

A calculation method linking the wear rate γ to specific pressures p and relative sliding velocity v of a friction pair was developed by A. Pronikov [52]. Two types of wear can occur: surface wear and frictional joint wear. Surface wear refers to the change in part size perpendicular to the friction surface Δh. This method allows the degree of wear and the shape of the worn surface to be determined based on the wear behaviour of materials and the joint configuration. It is important to note that the wear resistance factors K_1 and K_2 in the formula can only be determined through long-term experimentation, making wear calculations meaningless in advance.

Wear calculation model by Kragelsky et al.

In other fields of research, scientists use calculation methods that consider various factors, such as the structural characteristics of the friction pair, the physico-mechanical parameters of the friction material, and the geometrical parameters of the surface of the parts. Some notable scientists in this group are I. Kragelsky and N. Dyomkin. The calculation formulae take into account the elastic characteristics of the material, the

working mode of the part (load, speed), external conditions (lubrication, environment), structural features of the friction assembly, as well as non-standard roughness parameters such as coefficients b and v, radii of roughness surfaces, etc. These parameters add complexity to the wear calculations [53], [54], [57].

Wear calculation model by Rudzītis et al.

The wear calculation method used by J. Rudzītis and O. Linins is based on I. Kragelsky's wear calculation model, which has been expanded to include several important parameters. This allows the wear calculation equation to be applied to solve engineering problems. The wear process is divided into three stages: running-in wear (U_r), normal wear (U_n), and catastrophic wear. In the model, the wear value U_r for wear that occurs during the running-in stage is determined experimentally, while the wear value U_n for normal wear is calculated. This wear calculation method can be described as experimental-theoretical.

The formula for the calculation of linear wear for friction surfaces [50] by J. Rudzītis et al.:

$$E\{U_n\} \approx k_m \cdot K_R \cdot K_{F-M} \cdot \frac{q}{E} \cdot Ra \cdot \frac{L_b}{S_{m2}^a}. \tag{1.2}$$

where

k_m – coefficient depending on the parameters of the fatigue curve;

K_R – complex of surface roughness parameters;

K_{F-M} – complex of physico-mechanical parameters;

q – pressure acting on contacting surfaces;

L_b – friction path length;

E – modulus of elasticity of the material of the worn part;

Ra – arithmetic mean deviation of the roughness of the worn surface;

RSm_2^a – the average surface roughness step in the friction direction for the active surface.

1.2. Summary of approaches to wear determination

A comprehensive summary of known wear calculation models and approaches is presented in Table 1.1.

Table 1.1

Summary of the Literature Review on Wear Calculations

Reference	Theoretical background	Theoretical wear calculation	Experimental studies	Simulation of the wear process	Roughness profile parameters (2D)	Surface texture 3D) parameters	Notes
Xu Wujiao et al. [1]	Archard	+	Forward-back movement	-	-	-	The formula was improved
Adrians et al. [2]	Archard	+	-	Yes, FEM	-	-	The formula was improved
Reichert et al. [3]	Archard	+	-	Yes, FEM	-	-	The formula was improved
Wan-Gi Cha et al. [5]	Archard	-	Real object	Yes, FEM, REDSY	-	-	The formula was improved
Gao Deli et al. [6]	Archard	+	+	-	-	-	The formula was improved
Brandao et al. [7]	Archard	+	+	+	+	-	The formula was improved
Frischmuth et al. [10]	Archard	+	-	-	-	-	The formula was integrated into a mathematical model
Khader et al. [26]	Archard	+	+	+	-	-	The formula was improved
Dirks and Enblom [27]	Archard + Jendel	+	-	+	-	-	The formula was improved
Yuanpei Chen et al. [28]	Archard	+	-	+	-	-	The formula was improved
Yanfei Liu et al [40]	Archard	+	+	-	-	-	The formula was improved
Weijun Tao et al. [30]	Archard	+	+	-	-	-	The amount of wear is practically assessed by measuring the free movement of the parts
Popov et al. [31,32]	Archard	+	-	+	-	?	Archard and Rabinovich. Surface texture is shown but no parameters are defined.
Fei Lyu et al. [8]	Mixed	+	+	+	-	-	
Kloss et al. [11]	Mass balance and energy balance model	+	+	+	?	-	For wear calculations, data is taken from previous experiments
[13]–[15], [18]–[22], [24],	Determination of wear experimentally	-	+	-	-	-	The amount of wear is determined on the

[25]							basis of experimental results
Pronikov et.al. [52]	Pronikov	+	-	-	-	-	Wear is determined by the change in relative position of the aligned parts.
Kragelsky et al. [53], [54], [57]	Kragelsky	+	-	-	+/-	-	Non-standard surface roughness parameters are applied
Rudzītis et al. [50]	Rudzitis	+	-	-	+	-	Standardised surface roughness parameters (2D) are applied

1.3. Conclusions

There are two main approaches to determine wear, which are analytical wear calculation and experimental studies. However, experimental studies require specific equipment for the wear process and for the determination and analysis of wear values. Analytical wear calculation methods are still in use, but they often require coefficients/parameters that are determined by lengthy experiments, making the analytical calculations meaningless.

In modern scientific research, several methods of analytical wear calculation are still being used. Each method is based on the inclusion of certain dominant parameters in the calculation. However, the coefficients included in the wear calculation formulae have to be determined by lengthy experiments, which reduces the accuracy of the calculations.

A study by Kragelsky et al. showed that the wear calculation takes into account several parameters that operate in the real wear process; however, the friction surface is described by non-standardized roughness parameters and coefficients. On the other hand, the wear calculation model of Rudzitis et al. considers the standardized surface roughness profile parameters by modelling the surface microtopography with a separate section of probability theory – random field theory and friction surface destruction according to fatigue theory. This model can be considered a complete model for the calculation of friction surfaces at the moment. However, a major drawback is the use of surface roughness profile (2D) parameters, which do not provide complete information about the actual microtopography of the friction surfaces, resulting in reduced accuracy of the wear calculation.

Based on the literature review, **the following research hypothesis is put forward**: The introduction of surface texture (3D) parameters, as well as the refinement of individual material fatigue parameter's values in the sliding friction pair wear calculation, will increase the accuracy of the calculation by synthesising a new mathematical model for the wear calculation and developing a methodology for predicting the lifetime of the friction pair.

2. FRICTION SURFACE DESCRIPTION AND BASIC PRINCIPLES OF WEAR PROCESS ANALYSIS AND OPTIMISATION

This chapter discusses the model for contact between friction surfaces, its parameters, and an example of optimising the wear calculation formula's individual parameters.

2.1. Description of the friction surface, the contact model and its basic output parameters

The micro-topography of a friction surface, particularly in the case of irregular surface roughness, is quite complex. This is because the surface roughness asperities are located at different heights and have different shapes and configurations. Therefore, researchers are working to create a complete description of the rough surface profile.

When studying irregular surface roughness, the method of random function theory is effective. This means that surface microtopography can be described by a bivariate random function, which is a random field $h(x, y)$ with two variables: x and y [41], [50]. The random field at worn surfaces is assumed to be normal, which means that the ordinates of such a field are distributed according to the normal distribution law [50] and are characterized by the height parameter Sq – root mean square deviation from the midplane, μm.

An important characteristic of the random function is the *correlation function*, which indicates the relationship between the points of the random function. The correlation function depends on two variables: τ_1 and τ_2. These variables are projections onto the abscissa and ordinate axis of the vector τ, which connects two surface points in the Cartesian coordinate system. The faster the correlation function decreases, the more chaotic the random field [41].

In 2012 (ISO 25178-2:2012), a standard for surface texture (3D) parameters was introduced, which is considered one of the most significant scientific developments in product manufacturing and inspection. This standard has greatly impacted the approach to further research and manufacturing, improving the accuracy and quality of results achieved and providing ample opportunities to integrate the new parameters into research processing and analysis at a fundamental science level.

Several researchers, in their studies [35]–[40], [42], [59], have shown that surface texture (3D) parameters provide more detailed information about the real surface topography compared to 2D parameters, allowing for a more accurate analysis of results. This is an essential prerequisite for the Thesis.

Based on the above, the surface contact model considered integrates the 3D texture parameters that are necessary to define a rough surface. This model will be applied in the wear analytical calculations discussed below.

Based on the aforementioned information, we can establish an irregular frictional surface contact model: *surface roughness is described by a normal homogeneous random field h(x, y) of two variables, x and y, whose correlation function is continuous and has continuous derivatives*. The mean of this random field is represented by a plane, also known as the median plane [50], [51].

According to reference [50], after taking into account the aforementioned parameters and incorporating the 3D texture parameters into the surface description model, the following equation is derived:

$$Sa = \sqrt{\frac{2}{\pi}} Sq. \tag{2.1}$$

where *Sa* is the arithmetic mean deviation of the field from the median plane, μm.

In turn, $\rho(\tau_1, \tau_2)$ allows us to determine the corresponding roughness step parameters RSm_1 (step perpendicular to the machining direction along the midplane) and RSm_2 (step in the machining direction along the midplane) (Fig. 2.1).

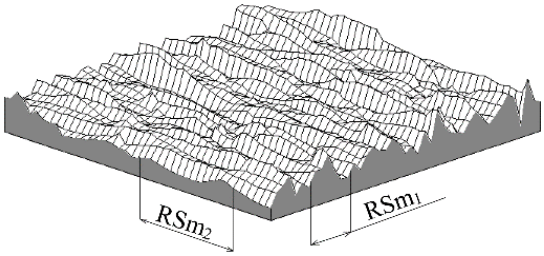

Fig. 2.1. Step parameters for irregular surface roughness [45].

The step parameters RS_{m1} and RS_{m2} allow the determination of the anisotropy coefficient *Str* [46]:

$$Str = \frac{RSm_1}{RSm_2} = \frac{n_2(0)}{n_1(0)}. \tag{2.2}$$

where $n_1(0)$ and $n_2(0)$ are the number of nulls in the *x* and *y* directions of the two mutually perpendicular directions (i.e., the transverse and longitudinal directions of the surface section).

In this way, a set of rough surface output parameters can be formulated: a rough surface can be described in height using the *Sa* parameter, and in steps – longitudinally with RSm_2 and transversally with RSm_1. The proposed surface texture (3D) parameters are technologically feasible in the surface preparation process and can be easily determined with modern measuring instruments such as *Mitutoyo FORMTRACER Avant* 3D, or analogues.

2.2. Mathematical model for wear calculation

The calculation process of the linear wear U_l (μm), can be described by the following formula [46]:

$$U_l = V_\Sigma \cdot \frac{N_{cf}}{N_c}. \tag{2.3}$$

where

V_Σ – the deformed volume over the entire friction surface;

N_{cf} – the actual number of cycles to which the surface asperities are subjected during the friction process;

N_c – the number of cycles leading to the destruction of the surface asperities.

The actual number of cycles N_{cf}, which deform surface asperities during the two-surface friction process, can be calculated as follows [45]:

$$N_{cf} = \frac{L_b}{RSm_2^a}. \tag{2.4}$$

where L_b is the length of the friction path, m; and RSm_2^a is the average surface roughness step in the direction of friction for the surface that causes abrasion on the other surface (i.e. the active surface), measured on a 3D surface, mm.

2.3. Detail's surface destruction model

Numerous studies have confirmed that the wear process is a result of fatigue [50], [51], [58]. This means that fatigue cracks are created and then propagate in the materials that make contact, eventually leading to the separation of material particles. The roughness of the contact surface generates stress that facilitates the destruction of the material, as shown in Fig. 2.2.

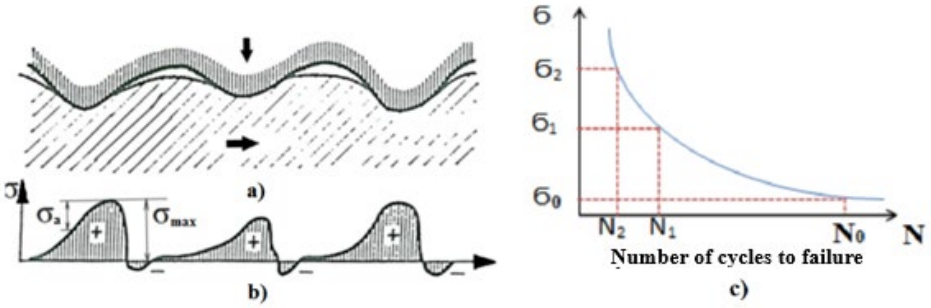

Fig. 2.2. a) Load diagram for the interaction of irregular rough surface asperities; b) stress change diagram; c) cycle number curve [45].

In reciprocal motion, any protrusion whose height exceeds a certain level, determined by the position of the opposite protrusion, deforms that protrusion, generating a stress field. Figure 2.2 shows the stress variation that occurs in tension-

compression following a non-symmetrical cycle. Based on [51], the number of cycles N_c for material failure can be determined as follows:

$$N_c = \frac{N_0}{5 \cdot m!} \cdot t_\sigma^m. \tag{2.5}$$

where

t_σ – the dimensionless stress ratio;

N_0 – number of cycles of the material under asymmetric loading according to the value of the endurance stresses σ_0 (Fig. 2.2 c));

m – the degree of the material fatigue curve equation for the wearing surface.

After considering [50], [51] and the previously mentioned relationships, the formula for determining the dimensionless stress ratio t_σ is:

$$t_\sigma = \frac{\sigma_0}{\sigma_a}. \tag{2.6}$$

where σ_0 is the limit of the material's endurance stresses, MPa, and σ_a is the stress amplitude, MPa.

Formula (2.6) is an important equation that takes into account the stress amplitude parameter, σ_a. This equation is based on the studies conducted by J. Rudzitis [65], [66] and G. Konrads [67]. The studies assume that the surface is deformed by high roughnesses caused by friction. The density of these roughnesses is a function of the degree [66], and they are considered to be above the level of $\gamma = 2$. With the right simplifications, the following relation can be obtained:

$$\sigma_a \approx \frac{\pi^2}{\sqrt{2}} \cdot \frac{E}{[K(e)]^{1/2}} \cdot \frac{Sa}{RSm_1}. \tag{2.7}$$

Formula (2.7) provides the average stress amplitude in friction for deformed irregularities. When we insert Eq. (2.7) into the basic Formula (2.5) for material failure, we get the final formula to calculate the number of cycles needed for the failure of a material on a wearing surface:

$$N_c = \frac{N_0}{5 \cdot m!} \cdot \left[\frac{\sqrt{2}}{\pi^2} \cdot \frac{\sigma_0 \cdot RSm_1 \cdot K(e)^{1/2}}{E \cdot Sa} \right]^m. \tag{2.8}$$

The resulting relationships allow the number of cycles required to break the material to be determined. For this purpose, the characteristics of the fatigue (*Weller*) curve N_0, m, σ_0 and the elastic modulus E of the material, as well as the roughness step in the transverse friction RSm_1 must be known.

2.4. Calculation of the particle volume of the abrasion process

Since the irregular surface roughness in the model is described by a normal random field $h(x, y)$, the high asperities of such a field can be described by elliptic paraboloids whose segment volume V_i is [58]:

$$V_i = \frac{\pi \cdot h_0^2}{K_i^{1/2}}. \tag{2.9}$$

where h_0 is the height of the paraboloid segment measured from the apex (thickness of the separated particle), mm, and K_i is the curvature of the i-th ridge of the roughness.

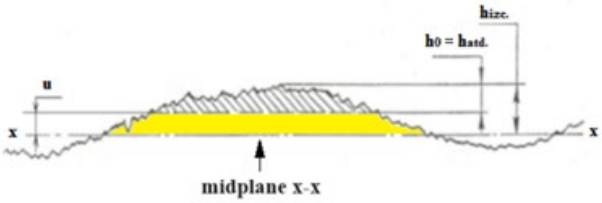

Fig. 2.3. Possible detachment of wear particles from a surface asperity [45].

The thickness of particles separated by abrasion depends on various physico-mechanical factors such as the condition of the surface layer and the size of the accumulation zone. As per the moving contact model, abrasion can follow a cyclic pattern where cracks develop in the subsurface layers due to the stress field from the load, causing them to grow and delaminate with a thickness h_{atd}. This value is estimated by analysing the overburden layer condition, assuming that $h_0 = h_{atd}$. The force causes the roughness deformation to reach a level u (the normalized value of the level u is $\gamma = u/Sq$). Based on mathematical calculations and analysing previous literature, the average value of the volume separated by one i-th asperity (V_i) can be determined.

After analysing the relationships obtained in the literature [50], [51] and performing mathematical calculations, the average volume separated by one i-th asperity (V_i) can be determined as follows:

$$V_i \approx \frac{Sq}{2 \cdot \gamma^2 \cdot \pi \cdot n_1(0) \cdot n_2(0)}. \tag{2.10}$$

To determine the total volume V_Σ separated by all the asperities, it is necessary to multiply the volume (V_i) of one asperity by the number of deformed asperities (N_γ).

2.5. Determination of the number of deformed asperities

In the abrasion process, the number of asperities on the surfaces in contact is a crucial parameter. The surface $h(x, y)$ is defined as the part of the rough surface above the level u, which is the height of the slit from the average field value. This is shown in Fig. 2.4. Unlike the profile, the splitting occurs along continuous curves. This can be seen in a simplified form in Fig. 2.4 b), which shows a top view of the bevelled surface.

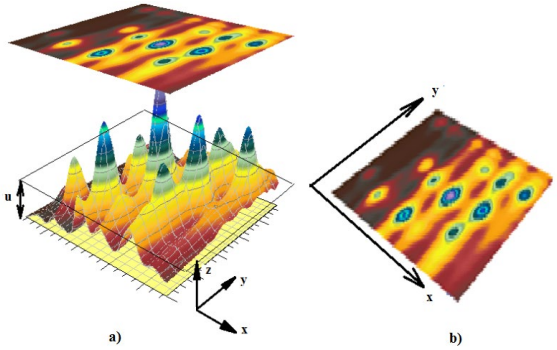

Fig. 2.4. Graphical representation of the number of surface asperities: a) – 3D surface slice at level u; b) – the slice of surface at level u viewed from above [47].

After conducting the aforementioned analysis and mathematical transformations, we can assume that the deformation occurs with higher roughness ($\gamma \geq 2$) and use the following formula to determine the number of asperitiess (N_γ) per unit area [47]:

$$N_\gamma = \frac{1}{5} \cdot n_1(0) \cdot n_2(0). \tag{2.11}$$

An experiment was conducted to verify the accuracy of the values obtained through the calculation of asperities using Formula (2.11). The experiment involved measuring a coated surface (Fig. 2.5) using a *Taylor Hobson Intra 50* surface texture measuring machine.

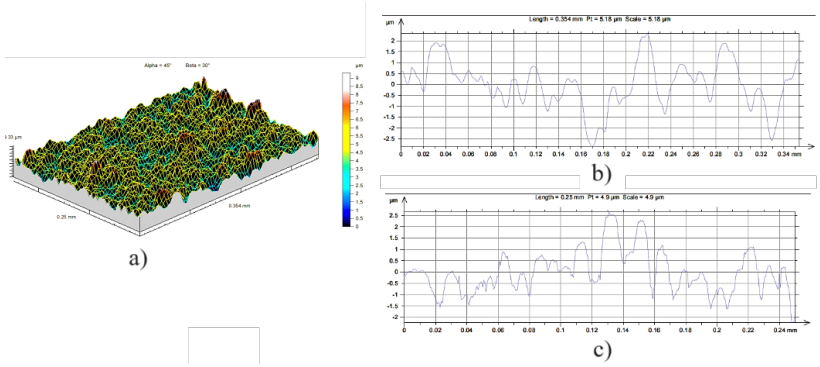

Fig. 2.5. Measurement of 3D surface texture roughness parameters: a) – 3D image of the surface; b) – profile in the x-axis direction (along the long edge of the sample); c) – profile in the y-axis direction (along the short edge of the sample) [47].

In this instance, the surface is characterised by the following main parameters: Sa = 0.811 µm; Sds = 11624 pks/mm^2 (number of asperities).

The number of nulls and the values required for theoretical calculations can be found using the profile parameters (Fig. 2.5 a), b)) that have been determined for the 3D surface: RSm_1 = 0.0253 mm; RSm_2 = 0.0166 mm.

To determine the number of asperities depending on the level u, the surface was cut at different levels, counting from the median plane. Examples of the slit at $u = 1Sq$, $u = 2Sq$, $u = 3Sq$ and $u = 4Sq$ are given in Fig. 2.6 [64].

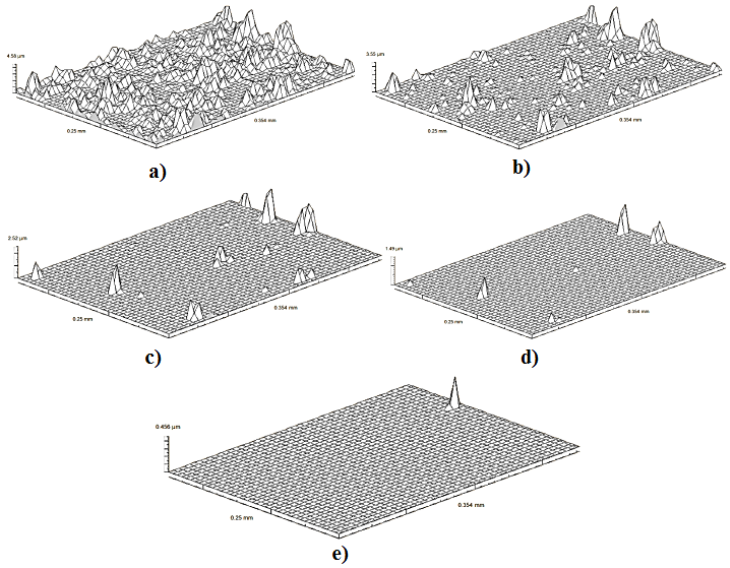

Fig. 2.6. Surface crossections at different levels:
a) – surface slice along the midline; b) – surface slice *1Sq* above the midline; c) – surface slice *2Sq* above the midline; d) – surface slice *3Sq* above the midline; e) – surface slice *4Sq* above the midline [47].

The results of the count measurements and the analytical calculations are summarised in Fig. 2.7.

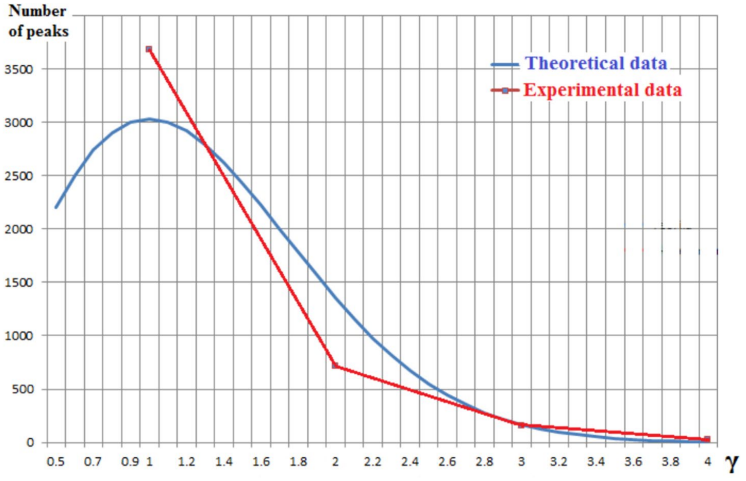

Fig. 2.7. Experimental and theoretical number of asperities [47].

In Fig. 2.7, it is observed that the number of surface roughnesses obtained from the calculation model at high gamma levels ($\gamma \geq 2.5$) is very similar to the experimental data. This suggests that the theoretical calculation formula can be used to calculate the number of surface roughnesses at $\gamma \geq 2.5$. Taking into account the mathematical calculations and expressing *Sq* from Formula (2.1), the cumulative volume per unit area of the surface roughnesses separated by friction can be calculated as follows:

$$V_{\Sigma} = \frac{Sa \cdot \sqrt{\pi}}{10 \cdot \sqrt{2} \cdot \pi \cdot \gamma^2}. \tag{2.12}$$

where V_i is the volume value of the *i*-th asperity separated andN_γ is the number of deformed asperities per unit area.

2.6. Summary of wear calculation's final formulae

Using Formula (2.3) and inserting Eqs. (2.4), (2.8), and (2.12) into it, we obtain the formula for the linear wear U_l calculation:

$$U_l = \frac{5 \cdot m!}{N_0} \cdot \frac{Sa \cdot \sqrt{\pi}}{10 \cdot \sqrt{2} \cdot \pi \cdot \gamma^2} \cdot \left(\frac{E}{\sigma_0}\right)^m \cdot \left(\frac{Sa}{RSm_1}\right)^m \cdot \left(\frac{\pi^2}{\sqrt{2} \cdot K(e)^{1/2}}\right)^m \cdot \frac{L_b}{RSm_2^a}. \tag{2.13}$$

In addition to the physico-mechanical parameters of the parts known above, Formula (2.23) contains parameter γ, which is determined in contact with the parts as the relative surface deformation rate. This level is determined for the surface subjected to wear using the contact theory Formulae [66]:

$$q = \frac{k_q \cdot Sa}{RSm_1 \cdot \theta} \cdot F_1(\gamma). \tag{2.14}$$

where

q – the load on the contacting surfaces, MPa;

k_q – a coefficient that depends on the rough surface anisotropy parameter *Str*;

$F_1(\gamma)$ – a function depending on the strain rate γ.

By expressing γ and carrying out mathematical transformations, we can relate the linear wear to the friction surface motion parameters, such as the sliding velocity (v) and movement time (t). This process results in a final formula that can be used to calculate the average linear wear (U_l) of a sliding friction pair:

$$U_l = 32 \cdot \frac{m!}{N_0 \cdot k_q^2} \cdot \frac{E^{m-2}}{\sigma_0^m} \cdot \frac{Sa^{m-1}}{RSm_1{}^{m-2}} \cdot \left(\frac{\pi^2}{\sqrt{2} \cdot K(e)^{1/2}}\right)^m \cdot q^2 \cdot \frac{v \cdot t}{RSm_2^a}. \tag{2.15}$$

where

m – the degree of the material fatigue curve equation of the worn part;

N_0 – number of cycles of the material strength of the worn component under asymmetric loading;

k_q – coefficient depending on the surface anisotropy parameter *Str*;

E – modulus of elasticity of the material of the worn part, MPa;

σ_0 – the limit of the material's endurance stresses, MPa;

Sa – arithmetic mean deviation of the wearing part from the midplane, μm;

RSm_1 – step perpendicular to the machining direction of the wearing surface, mm;

π – mathematical constant;

$K(e)$ – 1st order elliptic integral;

q – load applied to the worn component, MPa;

L_b – friction path, m;

RSm_2^a – the machining (or friction) step in the direction of the active surface, i.e., the surface contributing to the abrasion of the second surface, mm;

v – velocity of the friction pair relative to each other, m/s;

t – time of movement of the friction pair, s.

The linear rate of wear can be determined as follows:

$$V_{U_l} = \frac{U_l(t)}{t} = 32 \cdot \frac{m!}{N_0 \cdot k_q^2} \cdot \frac{E^{m-2}}{\sigma_0^m} \cdot \frac{Sa^{m-1}}{RSm_1^{m-2}} \cdot \left(\frac{\pi^2}{\sqrt{2} \cdot K(e)^{1/2}} \right)^m \cdot q^2 \cdot \frac{1}{RSm_2^a} \cdot v. \quad (2.16)$$

By knowing the linear wear and the rate of wear, one can determine the service life of a friction pair:

$$T = \frac{U_l}{V_{U_l}}. \quad (2.17)$$

It can be seen that Eqs. (2.15) and (2.16) involve the structural-kinematic characteristics of the friction pair, the fatigue characteristics of the friction pair component materials, the mechanical characteristic of the component material and the surface texture (3D) parameters.

It is not excluded that not only the effects of fatigue deformation but also abrasive, adhesive and other wear effects, as well as lubricant and temperature effects, may be at work in the wear process, resulting in quantitative wear values that may differ significantly from those proposed by this theory.

2.7. Parametric optimisation

In real mechanisms and machines, the maximum allowable wear (U_l) can be set. It is then possible to derive the friction pair life criterion T in different forms from the mathematical model (2.15) of the linear wear calculation and to consider the effects of several individual parameters. The example is based on data used in experimental studies on friction pairs (see Chapter 4), extending the range of values of the quantities to be studied within certain limits.

In this case, T is time as the optimisation criterion. In addition, a constant C is defined and fixed; x and y are taken as variable parameters, which are the two variable parameters from Formula (2.15).

1. Having analysed the effect of the parameters ***Sa*** and ***RSm*$_1$** on the service life and assuming that in this and the following cases $m = 4$ (for the material of the worn part), let us consider the given parameters (x, y) in the following form:

$$T = C_1 \cdot \frac{y^2}{x^3}. \tag{2.18}$$

where $x = Sa$; $y = RSm_1$.

To express T, we can use the following expression:

$$T = \frac{U_l \cdot N_0 \cdot k_q \cdot \sigma_0^m \cdot RSm_1^{m-2} \cdot RSm_2^a}{32 \cdot m! \cdot E^{m-2} \cdot Sa^{m-1} \cdot \left(\frac{\pi^2}{\sqrt{2} \cdot K(e)^{1/2}} \right)^m \cdot q^2 \cdot v}. \tag{2.19}$$

Numerical value of the constant C_1 assuming $N_0 = 5 \times 10^6$; $k_q = 0.15$; $q = 0.87$ MPa, $v = 450$ mm/s; $E = 1.15 \times 10^5$ MPa; $\sigma_0 = 300$ MPa; $Sa = 0.00083$ mm; $RSm_1 = 0.017$ mm; $RSm_2^a = 0.065$ mm:

$$C_1 = \frac{U_l \cdot N_0 \cdot k_q^2 \cdot \sigma_0^m \cdot RSm_2^a}{32 \cdot m! \cdot E^{m-2} \cdot \left(\frac{\pi^2}{\sqrt{2} \cdot K(e)^{1/2}} \right)^m \cdot q^2 \cdot v} = 1,772 \times 10^{-2} \text{ [mm·s]} \tag{2.20}$$

Limit values for parameters Sa and RSm_1: $Sa = 0.0002...0.002$ mm; $RSm_1 = 0.001...0,1$ mm.

Given Expression (2.18), T is calculated as follows:

$$T(Sa, RSm_1) = \frac{C_1 \cdot RSm_1^2}{Sa^3} = 22 \times 10^6 \text{ [s]} \tag{2.21}$$

The graph in Fig. 2.8 illustrates the maximum lifetime of a sliding friction pair that can be achieved for specific values of the parameters Sa and RSm_1.

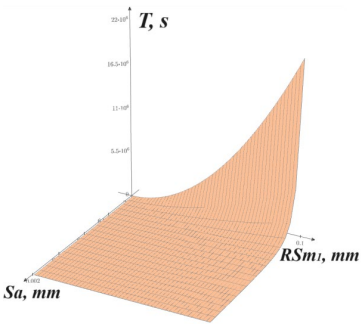

Fig. 2.8. Maximum lifetime extreme ($T = 22 \times 10^6$ s) with Sa and RSm_1 as variables.

According to the theory of extreme search in the two-parameter x, y-plane we can find partial derivatives of the criterion $\frac{\partial K}{\partial x}$ $\frac{\partial K}{\partial y}$ by each of the variables x and y:

$$\frac{d}{dx} C_1 \cdot \frac{y^2}{x^3} = \frac{-3 \cdot C_1 \cdot y^2}{x^4}. \tag{2.22}$$

$$\frac{d}{dy} C_1 \cdot \frac{y^2}{x^3} = \frac{2 \cdot C_1 \cdot y}{x^3}. \tag{2.23}$$

It follows from Expressions (2.22) and (2.23) that the derivatives of x and y as variables are of opposite signs, so that the optimum solution will be on the minimum and

maximum limits of the parameter: $x = x_{min}$, $y = y_{max}$, i.e., the lifetime of the sliding friction pair at Sa = 0.0002 mm and RSm_1 = 0.1 mm will be 2.2×10^7 seconds, i.e., 6111 hours.

An example of the visualisation of the friction pair lifetime calculation by analysing each parameter separately, i.e., assuming that Sa has the minimum value and RSm_1 has the maximum value, is shown in Fig. 2.9.

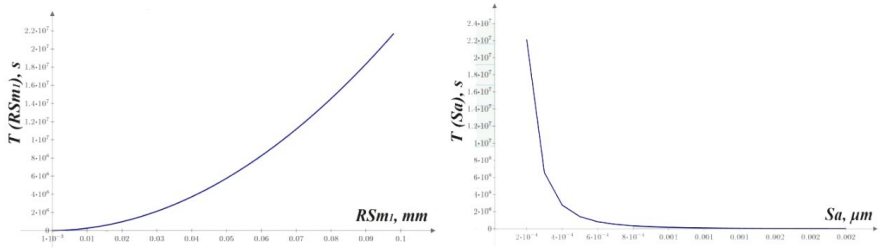

a) b)

Fig. 2.9. Lifetime of the sliding friction pair as a function of RSm_1 (a) and Sa (b).

The analysis shows that by ensuring that the values of the contact surface texture parameters Sa and RSm_1 of the contact parts are appropriate in the design process, i.e., by decreasing Sa and increasing RSm_1, it is possible to achieve a higher lifetime of the friction pair or to find optimum values at which a compromise between lifetime and surface texture parameters (Sa and RSm_1) will be achieved.

2. To analyse the effect of speed v and load $\boldsymbol{q}$ on service life, consider the given parameters (x, y) in the following form:

$$T = C_2 \frac{1}{x^2 \cdot y}. \tag{2.24}$$

where $x = q$ = 0.1...2.5 MPa;

$y = v$ = 100...1000 mm/s.

In this case, the constant $C_2 = 3.05 \times 10^6$ [mm·MPa^2].

Given Expression (2.37), T is calculated as follows:

$$T(q,v) = \frac{C_2}{q^2 \cdot v} = 3 \times 10^6 \text{ [s]} \tag{2.25}$$

The graph shown in Fig. 2.10 illustrates the maximum lifetime when varying the numerical values of q and v.

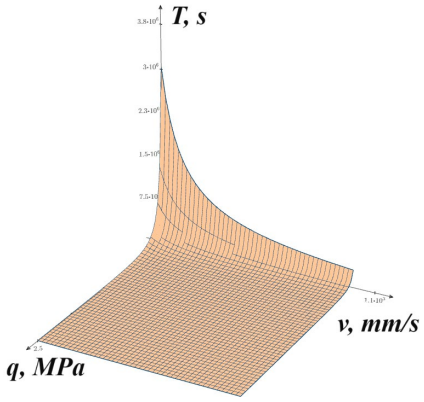

Fig. 2.10. Maximum lifetime extreme ($T = 3 \times 10^6$ s) with q and v as variables.

Partial derivatives of the criterion, $\frac{\partial K}{\partial x}\ \frac{\partial K}{\partial y}$ for each variable x and y:

$$\frac{d}{dx}\frac{C_2}{x^2 \cdot y} = \frac{-2 \cdot C_2}{x^3 \cdot y}. \tag{2.26}$$

$$\frac{d}{dx}\frac{C_2}{x^2 \cdot y} = \frac{-C_2}{x^2 \cdot y^2}. \tag{2.27}$$

It follows from Expressions (2.26) and (2.27) that the derivative of x and y as variables is negative in both cases, so the optimal solution will be on the minimum bounds of x and y: $x = x_{min}$, $y = y_{min}$, i.e., the sliding friction pair at $q = 0.1$ MPa and $v = 100$ mm/s will last 3×10^6 seconds, i.e., 833 hours.

An example of the visualisation of the friction pair lifetime calculation when the parameters q and v have a minimum value is shown in Fig. 2.11.

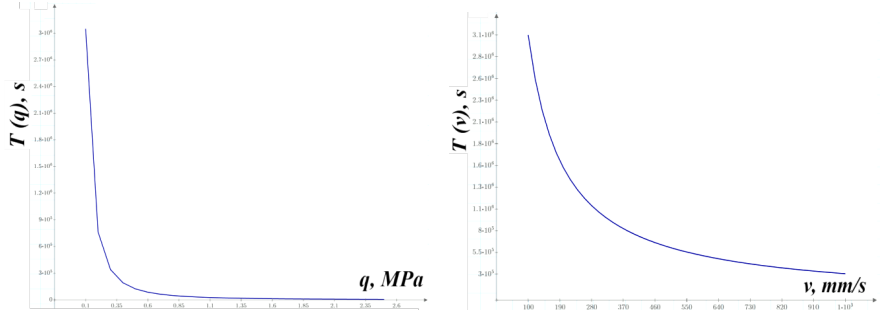

a) b)

Fig. 2.11. Lifetime of the sliding friction pair as a function of q (a) and v (b).

As can be seen, the maximum lifetime of a friction pair can be achieved under conditions where the sliding velocity (v) and the load (q) of the contact surfaces of the friction pair are reduced.

3. To analyse the effect of the parameters *Sa* and RSm_2^a on lifetime, consider the given parameters (*x, y*) in the following form:

$$T = C_3 \cdot \frac{y}{x^3}. \tag{2.28}$$

where $x = Sa$ = 0.0002...0.002 mm; $y = RSm_2^a$= 0.001...0.1 mm.

Constant $C_3 = 7.878 \times 10^{-5}$ [mm^2·s]

Given Expression (2.28), *T* is calculated as follows:

$$T(Sa, RSm_2^a) = \frac{C_3 \cdot RSm_2^a}{Sa^3} = 9{,}8 \times 10^5 [\text{s}]. \tag{2.29}$$

The graph in Fig. 2.12 illustrates the maximum lifetime when varying the numerical values of the parameters *Sa* and RSm_2^a.

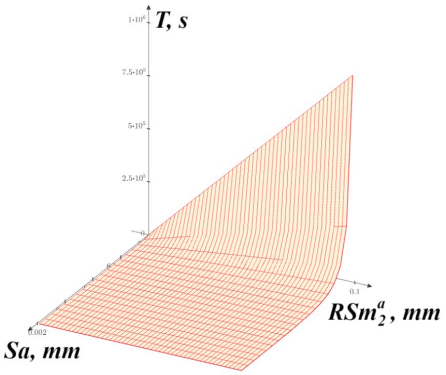

Fig. 2.12. Maximum lifetime extreme ($T = 9.8 \times 10^5$ s) with *Sa* and RSm_2^a as variables.

Partial derivatives of the criterion, $\frac{\partial K}{\partial x}\ \frac{\partial K}{\partial y}$ for each variable *x* and *y*:

$$\frac{d}{dx}\frac{C_3 \cdot y}{x^3} = \frac{-3 \cdot C_3 \cdot y}{x^4}. \tag{2.30}$$

$$\frac{d}{dy}\frac{C_3 \cdot y}{x^3} = \frac{C_3}{x^3}. \tag{2.31}$$

From Expressions (2.30) and (2.31), the derivatives of *x* and *y* as variables are of opposite signs, so that the optimal solution will be on the minimum and maximum boundaries of the parameter *x and y*: $x = x_{\min}$, $y = y_{\max}$, i.e., the sliding friction pair at Sa = 0.0002 mm and RSm_2^a = 0.1 mm will last 9.8×10^5 seconds, i.e., 272 hours.

An example of the visualisation of the friction pair lifetime calculation when Sa is the minimum value and RSm_2^a is the maximum value is shown in Fig. 2.13.

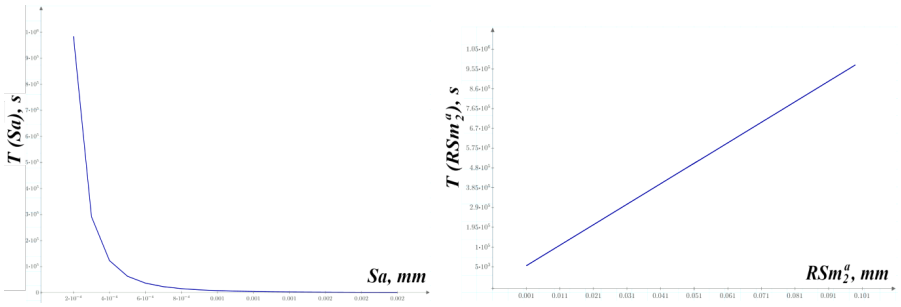

a) b)

Fig. 2.13. Lifetime of the sliding friction pair as a function of Sa (a) and RSm_2^a (b).

As in the option above, reducing Sa reduces wear, i.e., increases the service life. Increasing the pitch RSm_2^a of the friction surface that triggers wear also increases the service life, as the higher the pitch, the less frequent the impacts on the wearing surface (s) during movement.

2.8. Conclusions

1. In order to increase the lifetime of the friction pair, a parametric optimisation was performed using the developed analytical model for friction pair wear prediction, analysing the influence of surface texture (3D) parameters, speed and load on the lifetime of the friction pair.

2. It is concluded that by setting the service life as the main criterion and considering the 3D texture parameters and their different combinations, as well as the speed and load, it is possible to find the optimum parameter values at which the maximum service life of the sliding friction pair will be ensured at constant values of the other parameters included in the mathematical model for predicting the wear of the friction pair. The parametric optimisation analysis shows that by decreasing Sa, v, and q and increasing RSm_1 and RSm_2^a, it is possible to increase the lifetime of the friction pair or to find optimum values at which a compromise between the lifetime and the above parameters will be achieved.

3. By optimising the parameter values and seeing how they affect the wear rate, it is possible to select the appropriate surface texture (3D), load and speed parameters at the design stage that will ensure the lowest wear of the friction pair. Therefore, an analytical model for predicting the wear of a friction pair can be developed for both the direct task of calculating the predicted wear from known parameters and the inverse task of parametric optimisation to achieve maximum lifetime for a given friction pair.

3. THE FIRST PHASE OF EXPERIMENTAL STUDIES

This chapter describes the first stage of the feasibility experimental studies, which aim to verify the experimental results obtained from the analytical calculation Eq. (1.2) and to assess the suitability of the wear calculation model for solving practical engineering problems by performing wear prediction, which has not been done before.

3.1. Material selection and sample preparation

For the experimental studies, a roller-disc scheme was chosen to ensure the friction and wear process, which provides a convenient way to take the necessary measurements of the samples before and during the experiment.

The following samples were selected for the wear studies:

1) Cylindrical roller (Fig. 3.1) with a diameter of 6.5 mm for the contact surface; material – bronze (CuSn8, DIN 2.1030).
2) Disc diameter 100 mm, thickness 6 mm; material – steel (42Cr4, DIN 17212).

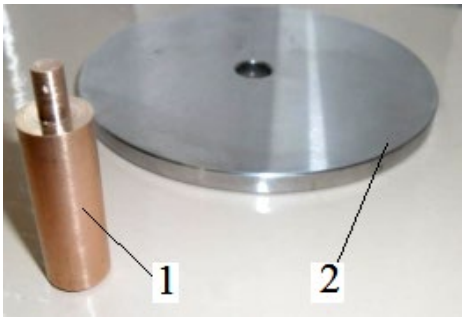

Fig. 3.1. Experimental samples.

The samples underwent a preparation process prior to the experiment to ensure that the contact surfaces had the required level of roughness. Following the grinding operations, surface roughness measurements were taken on both samples, in accordance with EN ISO 4287. Additionally, the length and mass of the bronze cylindrical roller were checked.

3.2. Equipment, instruments and software

The experimental studies of the wear process were conducted using a friction and wear research machine, designed by G. Spriņģis, the author of the Thesis. This machine is intended to solve the task of the Thesis and has a maximum specimen loading force of 300 N. It is also suitable for further research.

For the measurement of the friction force and the friction coefficient, a force measuring machine *PCE-FG50* with a measurement accuracy of 0.01 N (force

measurement limits 0...50 N) was used. The data of the measured parameters were collected using the data processing software *PCE-FG*.

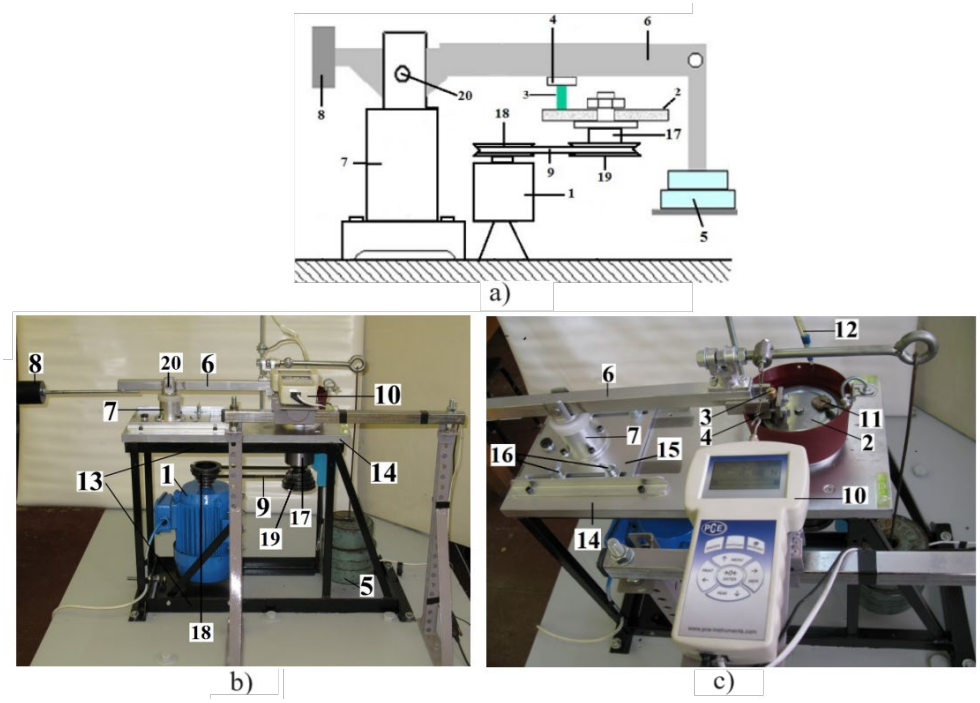

Fig. 3.2. Schematic diagram of the friction and abrasion process research machine: 1 – electric motor; 2 – rotating disc; 3 – press roller; 4 – press roller holder; 5 – slip weights; 6 –slip pendulum lever; 7 – slip pendulum locking axle bearing housing; 8 – weight; 9 – belt transmission; 10 – force measuring device *PCE-FG50*; 11 – oil spreader tube; 12 – oil feed channel; 13 – bearing frame; 14 – plate; 15 – tightening rocker arm moving plate; 16 – locating plate retainers; 17 – shaft bearing housing; 18 – driven pulley; 19 – driven pulley; 20 – tightening rocker arm pivot axis.

The required roughness parameters were measured using a *Taylor Hobson SURTRONIC 25* portable profilometer (*Taylor Hobson*, UK). A *Mitutoyo* digital micrometer (*Mitutoyo*, Japan) with an accuracy of 0.001 mm was used to control the length of the pressure roller before and at the appropriate stages of the experiment. The data obtained during the experiment was processed and analysed using *Microsoft Excel* and *MathCad*.

3.3. Sequence of experimental work and measurements

After the sample preparation, described in Section 3.1, both samples were fixed in the friction machine. Following the experimental feasibility work, the load q and the sliding speed v were selected and set (Table 3.1). Based on the fact that Formula (1.2)

requires the surface roughness parameters necessary for the calculation to be determined at the end of the running-in stage, the running-in process in the study was controlled by the settling of the friction coefficient (Fig. 3.3). After determining *Ra* and Sm_1 and adjusting the length of the bronze roller and determining its mass, the experiment was continued. The length of the bronze roller (also the mass for the control) was measured after a definite wear time, determining the experimental wear (Table 3.2).

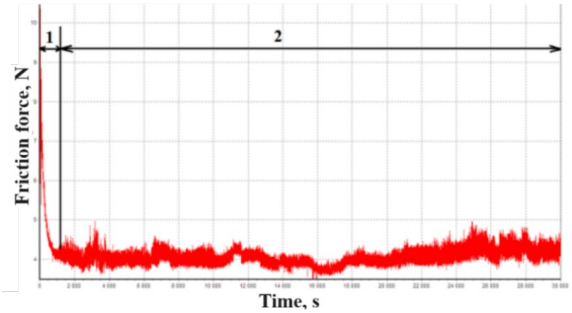

Fig. 3.3. Friction force over time:
1 – running-in period; 2 – normal wear period.

3.4. Processing and analysis of experimental data and analytical calculations

The values used in the experiment and the analytical calculations are summarised in Table 3.1.

Table 3.1

Set Values and Surface Roughness Parameters in the Experimental Study after Running-in Stage

Parameter		Designation	Numeric value	Unit
Load		q	11	MPa
Sliding speed		v	5000	mm/s
Fatigue failure parameters of the roller's (bronze, CuSn8) material	Degree of material fatigue curve equation	m	4	-
	Limit of resistance of the material at a symmetrical load cycle	σ_{-1}	150	MPa
	Number of loading cycles	N_0	5×10^6	-
Modulus of elasticity of the roller's material		E	1.15×10^6	MPa
Surface roughness parameters (after running-in stage)	Arithmetic mean deviation of surface roughness	Ra	0.6	µm
	Average step of the wearing part of the roller	Sm_1	0.060	mm
935820	Average step of the wear activating disc's surface	Sm_2^a	0.5	mm
Wear after running-in stage		U_p	7	µm

The calculated values of linear wear are summarised in Table 3.2, and the wear illustrating curves are shown in Fig. 3.4.

Table 3.2

Experimental and Analytically Calculated Linear Wear

Measurement No.	Time, hours	Experimental average wear after running-in stage, µm	Average wear (theory), µm
After running-in stage (16 hours), wear value 7 µm			
1	28	1.2	4.6
2	56	3.1	9.5
3	100	5.4	17.0
4	162	76	27.5
5	244	10.2	41.4

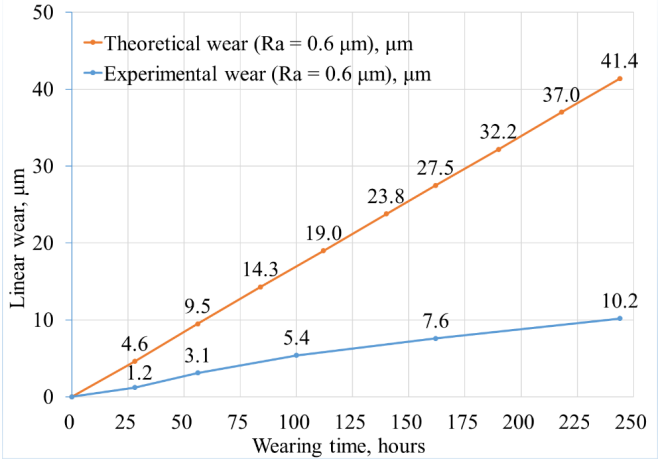

Fig. 3.4. Comparison of experimental and theoretical average values of linear wear (running-in period excluded).

The running-in stage for a given friction pair takes 16 hours. After this period, the wear for a normal (stable) period is calculated. An experimental time of 244 hours (friction path of 4392 km) is used to calculate normal wear. Figure 3.4 shows the blue curve, which represents experimentally obtained linear wear values, and the orange line, which represents the theoretical linear wear calculated using Formula (1.2). At the end of the experiment, the difference between the theoretical and experimental wear values is a factor of 4. However, 2D roughness parameters in Formula (1.2) do not always give a complete picture of the actual micro-topography of the friction surface. To demonstrate how roughness parameters affect wear calculations, additional values of *Ra* and Sm_1 were artificially chosen. The purpose of this analysis is not to find the closest value of a given parameter that matches the experimental wear data and the theoretically calculated values, but rather to show the influence of a given parameter on the variation of the wear curve and the importance of this parameter for the accurate

determination of the contact surface of the wear part of a friction pair as a result of the measurements (Fig. 3.5).

It is observed that the wear decreases with a decrease in the value of *Ra*, as shown in Fig. 3.5 a). The wear values obtained from the calculations show the closest agreement with the experimental data when *Ra* is at 0.4 μm. The difference between the results at the end of the wear stage is not more than 20 % at this value of *Ra*. For instance, reducing the value of *Ra* from 0.6 μm to 0.5 μm results in a 52 % decrease in the analytically calculated wear value, and the difference with the experimental data is 50 %. Conversely, increasing the value of *Ra* leads to an increase in the analytically calculated wear value.

After analysing the graph (Fig. 3.5 b)), it can be concluded that as the average step Sm_1 of the wearing surface increases, the wear decreases. This means that the higher the step, the rougher the friction surface and the more resistant it is to deformation. In the experiment, the value of Sm_1 was found to be 0.06 mm. Upon calculating the wear on a friction surface with this value, it was observed that the experimental and theoretical wear values at the end of the experiment differed by a factor of 4. However, assuming an increase of 0.01 mm in the value of Sm_1, the difference between the experimental and theoretical wear values decreased slightly more than two times. It should be noted that as the value of Sm_1 is increased, the wear also increases rapidly.

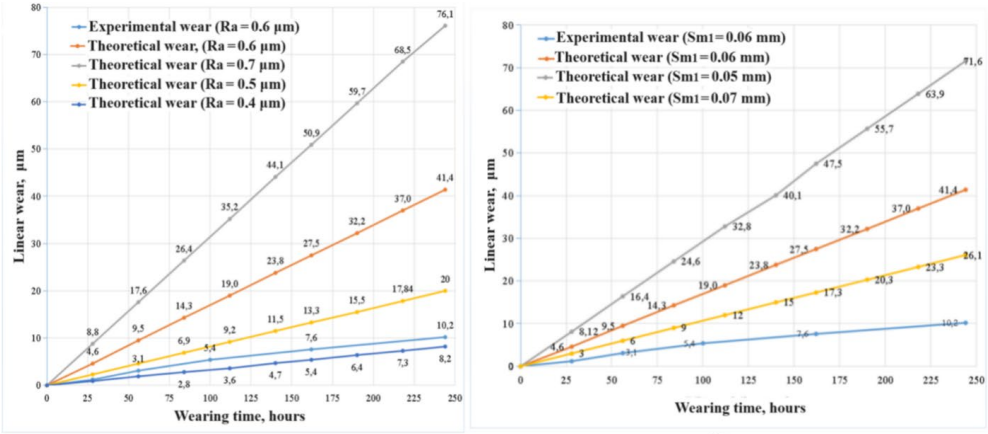

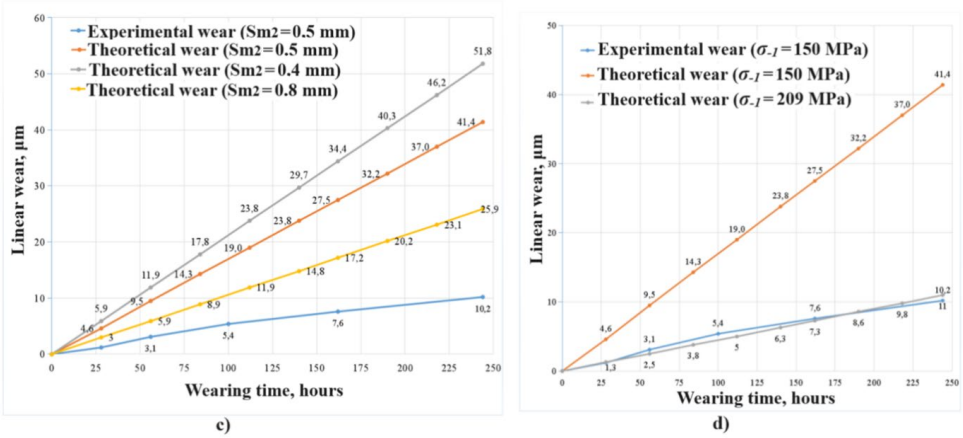

Fig. 3.5. Effect of surface roughness parameters and material ultimate stress σ_{-1} on linear wear: a) – effect of Ra; b) – effect of Sm_1; c) – effect of Sm_2^a; d) – effect of σ_{-1} (running-in period excluded).

The effect of changing the value of the step Sm_2^a (Fig. 3.5 c)) on the amount of wear is that the larger the step, the less frequent the impacts on the worn surface roughness during the sliding friction pair motion, and thus the less wear will be.

Analysing Fig. 3.5 a), b), c), it can be seen that the roughness parameters of the contacting surfaces of the friction pair have a significant influence, which justifies the need to determine the values of these parameters as accurately as possible during the measurements.

It is important to note that the friction surface parameters Ra, Sm_1 and Sm_2^a are interrelated, i.e., changing one parameter automatically changes the others, which was not considered in this analysis to show the effect of each parameter taken individually on the overall wear process and cumulative wear.

Figure 3.5 d illustrates the effect of a change in the numerical value of the material ultimate strength σ_r on the analytically calculated wear value. Based on Formula (1.22) for the wear calculated by J. Rudzītis, $\sigma_r = \sigma_{-1}$. For a given bronze material, the value of σ_{-1} is 150 MPa at symmetrical cycling. According to G.Spriņģis (the author of the Thesis), this type of sliding friction results in asymmetric loading of the surface bumps. In this case, $\sigma_r = \sigma_0$. The value of σ_0 for a non-symmetric cycle is 209 MPa. As can be seen from the graph shown in Fig. 3.5 d), at the stresses prescribed for the unsymmetrical loading case, the agreement of the wear values is close to 93 %. The higher the σ_r, the higher the fatigue resistance of the material and the lower the wear, which is also shown by the grey curve in the graph (Fig. 3.10).

3.5. Conclusions

1. The mathematical model of J. Rudzītis, Formula (1.2), for calculating friction surface wear has been experimentally validated for the first time. The analysis of the results of the experimental studies of the first phase has concluded that relatively small changes in the 2D roughness parameters of the surface and refinement of the material's strength limit parameter σ_r have a significant effect on the theoretically calculated values of wear.

2. It is concluded that the basic approach of the mathematical model, Formula (1.2) for calculating the wear of friction surfaces by J. Rudzitis provides an adequate algorithm of prediction of the wear, although significant deviations have been found from the real (experimentally determined) wear values.

3. To achieve greater accuracy in wear calculations, it is important to integrate 3D surface texture parameters instead of relying solely on 2D roughness parameters. This is because the latter are not perfect descriptors of the real surface's microtopography, and small variations in their values – which may occur depending on the measured profile track – can have a considerable impact on the results of the wear calculations. 3D surface texture parameters provide a more complete and accurate description of the 3D friction surface, making them a more reliable tool for accurate wear calculations.

4. The mathematical model, Formula (1.2), for the calculation of frictional surface wear assumes that the surface roughness is loaded symmetrically so that the strength limit at symmetric cycling is $\sigma_r = \sigma_{-1}$. However, the author of the Thesis suggests that in the case of tension-compression, the surface roughness is loaded unsymmetrically during tension, and thus $\sigma_r = \sigma_0$ can be assumed.

5. The author's new synthesised friction surface wear calculation model, including the 3D surface texture standardised parameters and the material fatigue wear parameters, was experimentally validated in the second phase of experimental studies (see Chapter 4).

4. THE SECOND PHASE OF EXPERIMENTAL STUDIES

This chapter describes the second phase of experimental studies. Its purpose is to verify analytically calculated wear values using a newly synthesised friction surface wear calculation model and compare the results with those obtained in the experimental studies.

4.1. Selection and preparation of samples

The scheme chosen for the wear studies is a "ball with ground contact plane – rotating disc".

The following specimens and their materials were selected for the experiment:

1. A steel ball (Fig. 4.1) with a diameter of 6 mm. The ball's material – 102Cr6 (EN 1.2067), hardness HRC ~ 63. The ball was machined before the experiment by grinding to obtain a plane with an area of ~ 2.1 mm.

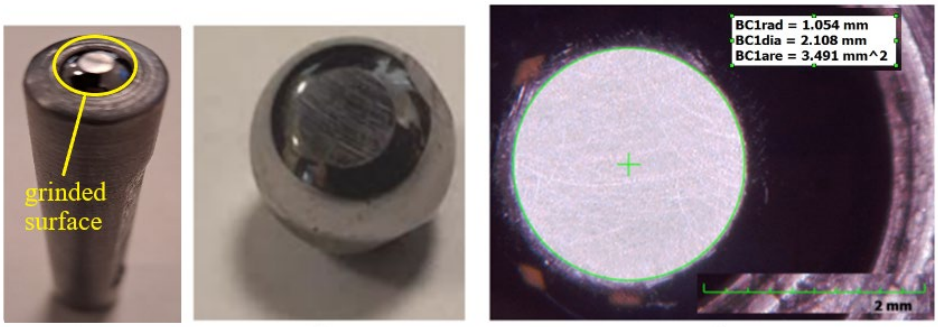

Fig. 4.1. A ball with a polished surface:
a) – ball in holder; b) – the ball's close-up; c) – sample measurement of the diameter and area of the polished surface of the ball.

2. A bronze disc with a diameter of 40 mm and a thickness of 5.5 mm. The surface of the disc was sanded with sandpaper with different gradations of abrasive grains until a surface of $Sa < 0.1$ was achieved.

The materials of the disc samples:

1) Group 1 bronze CW456K (EN 12164);
2) Group 2 bronze CW307G (EN 12163).

Before the experiment, the contact surfaces of all samples were treated with sandpaper with different abrasive grain gradations, ensuring $Sa < 0.1$. After the surface grinding operations were completed, all samples were cleaned with a wipe soaked in acetone to remove metal chips and abrasive from the sandpaper and subjected to control measurements of surface texture (3D) parameters according to EN ISO 25178.

4.2. Sequence of work, measurements and experimental procedures

After appropriately preparing the sample surfaces, the ball and the bronze disc samples were fixed in the tribometer fixtures. Three combinations of sliding speed (v) and load (q) values were selected considering the experimental feasibility work carried out previously, which can be found in Table 4.1. Five experiments for each set parameter group (definite load q and speed v) were conducted using a *CSM Tribometer* (*CSM Tribometer*, Switzerland) to study the bronze disc's material wear. Tables 4.2 and 4.3 summarise the average values of the measured surface parameters, along with the values required for the experiment and the calculation. To avoid overlapping of the curves in the plots of the wear results, the average values were calculated from the data of the five experiments for each combination of the set parameters. These values are then plotted in the form of wear curves.

Table 4.1

Parameters and Values for Experimental Studies

Option No.	**Parameter**				**Running-in stage, m**	**Total friction distance after running-in stage, m**
	Speed v, m/s	**Normal force F, N**	**Load q, MPa**	**Ball's diameter, mm**		
1	0.7	2	0.58	2.1	500	6000
2	0.45	3	0.87	2.1	1000	4000
3	0.3	5	1.45	2.1	1500	4000

During the running-in process, the contact surfaces of the friction couple are subject to various factors that cause rapid changes in the surface parameters involved in the abrasion process, until the friction process stabilises. Therefore, the measurement of the surface texture (3D) parameters of both specimens using the 3D contour and surface texture measurement system *Mitutoyo FORMTRACER Avant 3D* (*Mitutoyo*, Japan) was carried out only after the running-in stage had finished. Eq. (2.15) is generally applicable for wear calculations at any point during the wear process. However, it is recommended to measure surface texture (3D) after the running-in stage is completed due to the rapid change of surface roughness parameters during this stage. The duration of the running-in period during the experiment was determined by the stabilisation of the friction coefficient, which could be controlled by the data processing software *InstrumX* (Fig. 4.2).

Fig. 4.2. Determination of the wear process parameters.

The duration of the experimental period for different combinations of speed (v) and load (q) is presented in Table 4.1.

The wear values were monitored after every 500 meters of friction using a *Mitutoyo SURFTEST SJ-500* profilometer (*Mitutoyo*, Japan) to measure the width and cross-sectional area of the worn track. Further processing and analysis of the data obtained during the experiment were done using data processing software such as *TalyMap Gold*, *MCube Map Ultimate 8*, *MathCad,* and *Microsoft Excel.*

4.3. Processing and analysis of experimental data and analytical calculations for the friction pair steel (102Cr6) – bronze (CW456K)

The data obtained from the experiment and required for the analytical calculations based on Formula (2.15) for the friction pair steel (102Cr6) – bronze (CW456K) – are summarised in Table 4.2. In this particular case (unlike in the experimental studies of the first phase), it is assumed that the steel ball wears minimally, and the bronze disc is subjected to intense wear. Therefore, the wear of the steel ball is not analysed in this study.

Table 4.2

The Values, Material Properties and Surface Texture (3D) Parameters Set in the Experimental Study for the 1st Group of Samples

Option No.	**Speed *v*, m/s**	**Load *q*, MPa**	**Average values of surface texture (3D) parameters after running-in stage**			**Average wear after running-in stage, µm**
			Arithmetic mean deviation of surface roughness *Sa*, µm	**Average step of the worn component (disc) *RSm*$_1$, mm**	**Average step of the wear activating surface (ball) RSm_2^a, mm**	
1	0.7	0.58	0.59	0.016	0.092	2.86
2	0.45	0.87	0.62	0.032	0.088	4.40
3	0.3	1.45	1.5	0.034	0.11	4.50
Before the experiment			0.06	0.015		-
Degree of material fatigue curve equation *m*						4
Strength limit of the material at asymmetric load cycle σ_0, MPa						225
Number of resistance cycles of the material N_0						5×10^6
Modulus of elasticity of disc's material *E*, MPa						1.18×10^5
Surface anisotropy parameter *Str*						~ 0.03

Surface texture (3D) measurements were taken for the surfaces of the friction pair in accordance with EN ISO 25178. The average measurements for each variation of the selected speed (*v*) and load (*q)* are presented in Table 4.2, and a sample of the measurements is illustrated in Figs. 4.3, 4.4, and 4.5. The processed data array and surface visualisation (Fig. 4.3) revealed that the bronze disc displayed visible grooves in the friction direction after running-in stage, resulting in an average surface anisotropy coefficient value *Str* of less than 0.1 in this particular case.

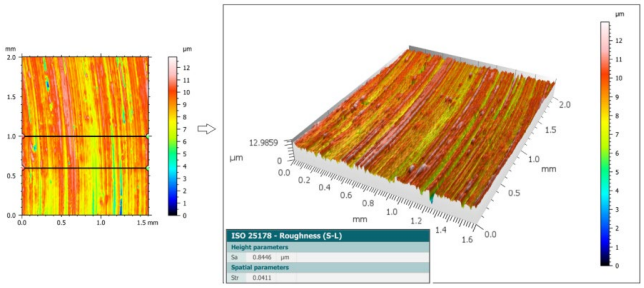

Fig. 4.3. Surface texture (3D) parameters' measurement of the disc after running-in stage (v = 0.7 m/s and q = 0.58 MPa).

The bronze disc's average step RSm_1 is measured across the friction direction from the 3D surface to facilitate further analytical calculations (see Fig. 4.4).

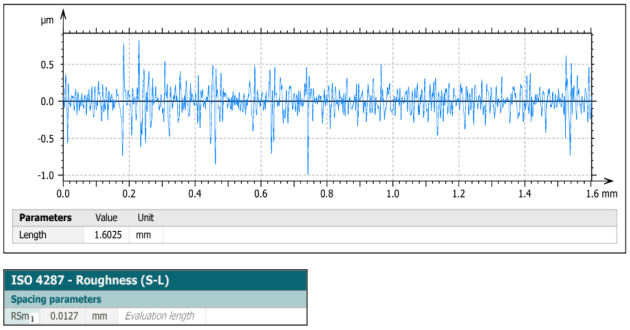

Fig. 4.4. Average step RSm_1 measurement of the bronze disc after running-in stage (v = 0.7 m/s and q = 0.58 MPa).

In Fig. 4.4, it can be seen that the step RSm_1 across the direction of friction for a given measurement is 0.0127 mm. On the other hand, Table 4.2 displays the average values of step for five samples, with three measurements per sample. Figure 4.5 provides an illustrative image of the grinded ball's surface (a), an example of the friction trace (b), and the results of the measurement of the required surface texture (3D) parameters (c).

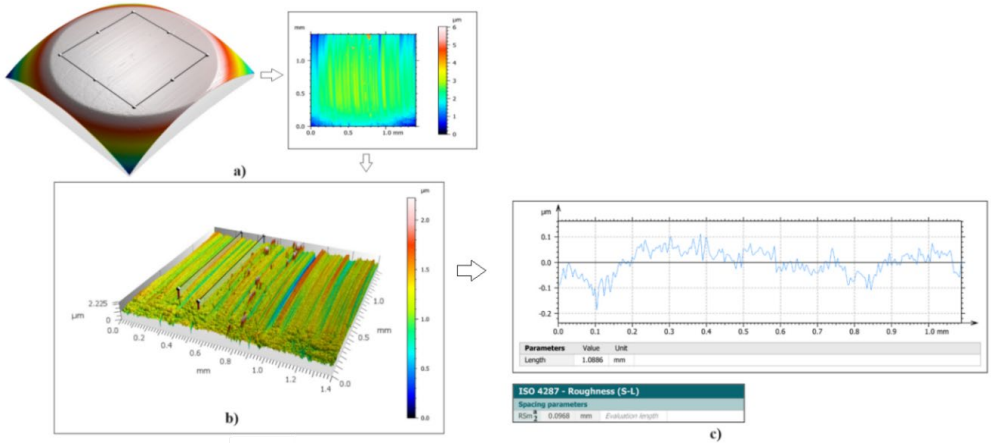

Fig. 4.5. Grinded ball's surface (a), friction trace (b) and measurement of the mean step RSm_2^a of the wear activating (the ball's) surface (c), (v = 0.7 m/s and q = 0.58 MPa).

In this particular measurement, the recorded value is 0.0968 mm. Table 4.2. displays the average value of the step RSm_2^a from measuring five samples. Each sample had a step measured at three points.

During the experiments, wear values were monitored every 500 meters of friction. The measurement results were then processed using *TalyMap Gold* software to determine the cross-sectional area of the worn track. At each wear measurement, the cross-sectional area of the worn track on the disc was measured at four locations (every

90°), and the average linear wear of the four measurements was calculated for each sample.

The cross-sectional area of the worn track, shown in red, is 14491 μm² (Fig. 4.6). Even though the measured area is irregular in shape, it is assumed that the linear wear will be calculated for a rectangle with side lengths *a* and *b*, for simplicity. Knowing the diameter of the ball, which coincides with the side *a* of the assumed rectangle of the worn track at a given friction path, the linear wear resulting from the experiment can be calculated.

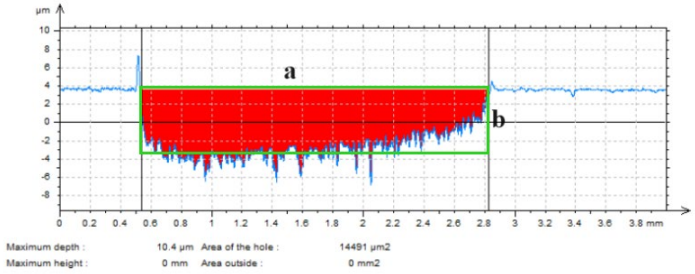

Fig. 4.6. Measurement of the cross-sectional area of the worn track on the bronze disc after 3000 m of sliding distance (v = 0.7 m/s, q = 0.58 MPa).

The graph presented in Fig. 4.7 displays the linear wear values obtained from both experimental and analytical calculations when v = 0.7 m/s and q = 0.58 MPa. This and the following graphs show the normal wear period (excluding running-in period).

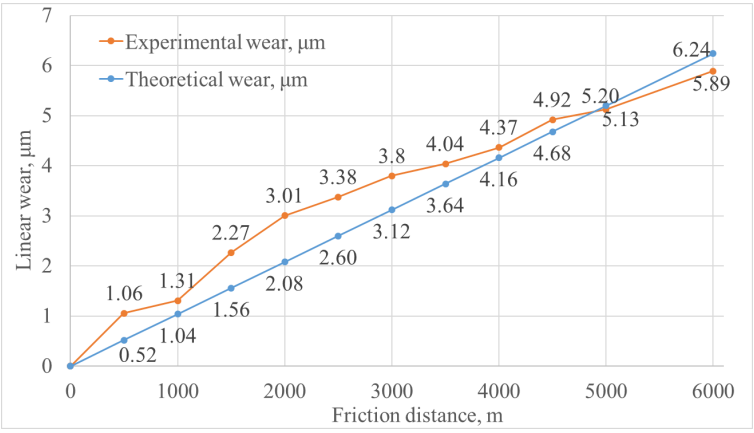

Fig. 4.7. Experimental and theoretical mean values of linear wear for the 1st group of samples (v = 0.7 m/s, q = 0.58 MPa)

Figure 4.7 indicates that the closest agreement between the experimental and analytically calculated wear values for the sliding friction pair is observed beginning from 4000 m of sliding distance. At 5000 m, the difference between the analytical and experimental wear values is only 1.3 %, while at 4500 m, it is 4.9 %. On average, the

variation between the experimental and theoretical wear values during the experiment does not exceed 18.3 %. The total theoretical linear wear, excluding the application, is 6.24 μm, and the experimental is 5.89 μm, which means that the difference in results after 6000 m is less than 5.6 %.

The friction coefficient's stabilisation process was determined after 1500 m, and the given limit value of the friction path was taken at the end of the running-in process. However, it should be noted that fluctuations in the friction coefficient were observed for some specimens during subsequent experiments. These fluctuations may indicate cyclic variations of wear parameters within certain limits, which may explain the difference between experimental and theoretical wear values.

The wear values at v = 0.45 m/s and q = 0.87 MPa are shown in Fig. 4.8.

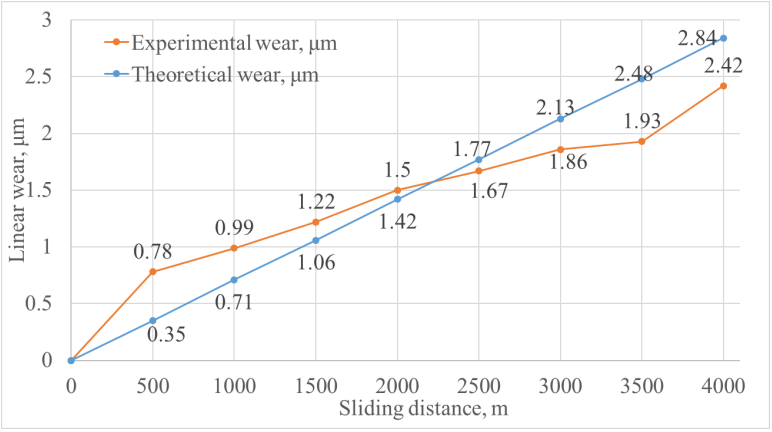

Fig. 4.8. Experimental and theoretical mean values of linear wear for the 1st group of samples (v = 0.45 m/s, q = 0.87 MPa).

It has been observed that the experimental wear values are higher than the analytically calculated values until the friction path reaches 2250 m. However, after 2250 m, the curve of wear values indicates that the experimental values become lower than the analytically calculated values. The intersection of the experimental and analytical wear curves occurs at 2250 m, while the closest agreement is observed at 2000 m and 2500 m of friction, reaching 94 %. The largest differences in wear values are observed at 500 m, which can be explained by the changing values of the parameters during the wear process for a given friction pair, as well as the possible continuation of the running-in period. The total theoretical linear wear at the end of the experiment, excluding the running-in period, is 2.84 μm, and the experimental wear is 2.18 μm. Comparing the two values, the difference does not exceed the 15 % limit.

Furthermore, the graph in Fig. 4.9 displays the wear values for the third parameter option, which includes the lowest speed (v = 0.3 m/s) and the highest load (q = 1.45 MPa). In this case, the variation between the experimental and theoretical wear values during the experiment does not exceed 10 % on average. The total calculated linear wear, excluding the running-in stage, is 78.87 μm, and the experimental wear is 81.98

μm, which means that the difference in values does not exceed –3.8 %. After analysing the data shown in Fig. 4.9, it can be concluded that, for the given parameters, the deviation between the theoretical and experimental wear values is the smallest compared to the cases considered above.

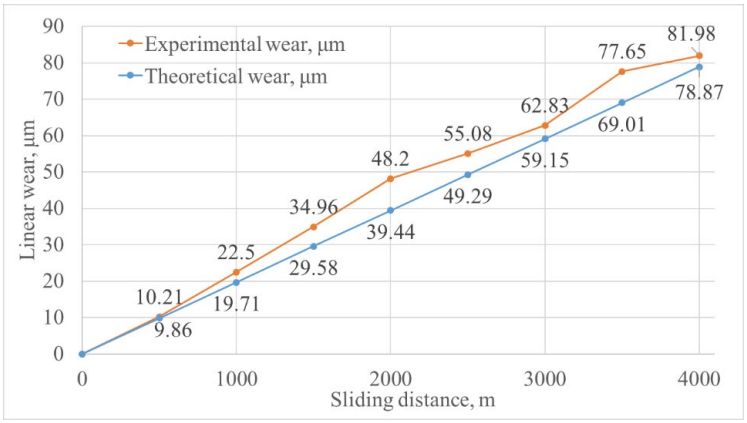

Fig. 4.9. Experimental and theoretical mean values of linear wear for the 1st group of samples (v = 0.3 m/s, q = 1.45 MPa).

4.4. Processing and analysis of experimental data and analytical calculations for the friction pair steel (102Cr6) – bronze (CW307G)

The experimental parameters, values obtained from the measurements and used in subsequent analytical wear calculations are listed in Table 4.3.

Table 4.3

The Values, Material Properties and Surface Texture (3D) Parameters Set in the Experimental Study for the 2nd Group of Samples

Option No.	**Speed v, m/s**	**Load q, MPa**	**Average values of surface texture (3D) parameters after running-in stage**			**Average wear after running-in period, μm**
			Arithmetic mean deviation of surface roughness Sa, μm	**Average step of the worn component (disc) RSm_1, mm**	**Average step of the wear activating surface (ball) RSm_2^a, mm**	
1	0.7	0.58	0.79	0.012	0.060	1.7
2	0.45	0.87	0.83	0.017	0.065	2.88
3	0.3	1.45	1.70	0.035	0.170	5.44
Before the experiment			0.06	0.015		-
Degree of material fatigue curve equation m						4
Strength limit of the material at asymmetric load cycle σ_0, MPa						300
Number of resistance cycles of the material N_0						5×10^6
Modulus of elasticity of disc material E, MPa						1.15×10^5
Surface anisotropy parameter Str						~0.03

Figure 4.10 shows the experimental and analytically calculated linear wear values for a given combination of materials at v = 0.7 m/s, q = 0.58 MPa.

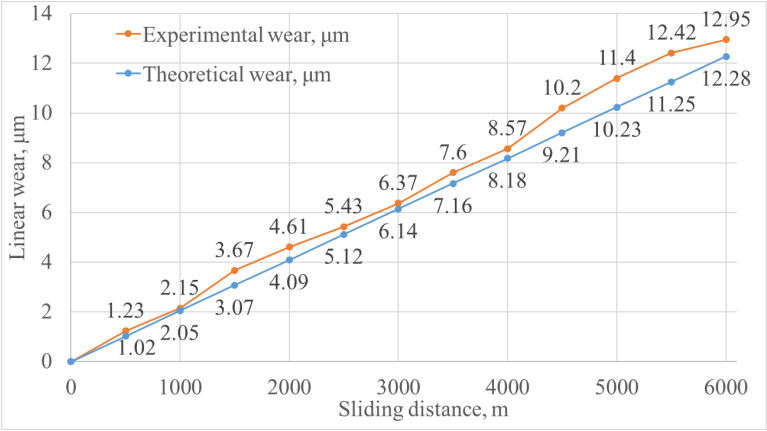

Fig. 4.10. Experimental and theoretical mean values of linear wear for the 2nd group of samples (v = 0.7 m/s, q = 0.58 MPa).

The graph in Fig. 4.10 indicates that the difference between the experimentally determined and analytically calculated values of linear wear doesn't surpass the 5 % limit at 1000 m, 3000 m, and 4000 m of friction. At 2500 m, 3500 m, and 6000 m, the difference doesn't exceed the 6 % limit. During the experiment, the variation between the theoretical and experimental wear values doesn't exceed 8.6 % on average. At the end of the experiment, the comparison between the analytically calculated and experimentally obtained wear values shows that it doesn't exceed the 5.2 % limit.

The wear values at v = 0.45 m/s and q = 0.87 MPa are illustrated in Fig. 4.11.

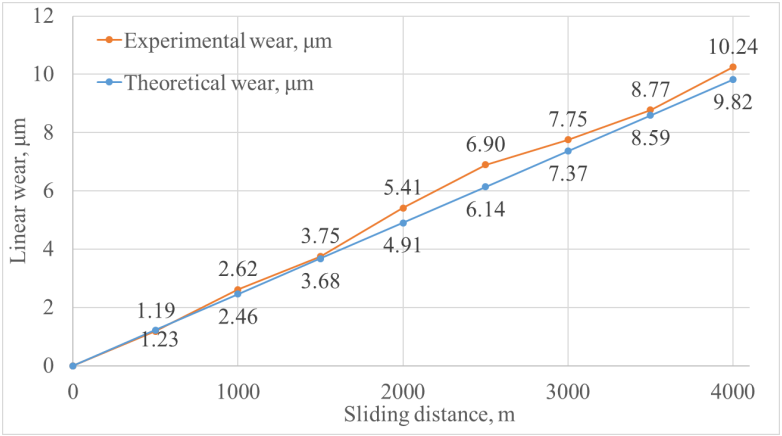

Fig. 4.11. Experimental and theoretical linear wear averages for the 2nd group of samples (v = 0.45 m/s, q = 0.87 MPa).

An analysis of the wear curves presented in Fig. 4.11 indicates that the theoretical and experimental wear values are closest at 1500 m (with a difference not exceeding 2 %) and 3500 m (with a difference not exceeding 2.2 %). On average, the variation between the experimental and theoretical wear values during the experiment does not exceed 5.4 %. At the end of the experiment, after 4000 m of friction, the difference in wear values is no more than 4.2 %, which is only 0.42 μm.

Figure 4.12 illustrates the linear wear values for a given combination of materials at $v = 0.3$ m/s and $q = 1.45$ MPa, both experimentally and theoretically.

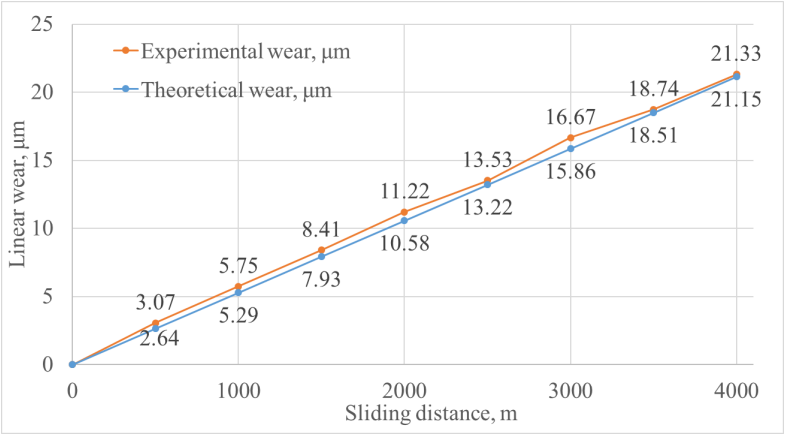

Fig. 4.12. Experimental and theoretical linear wear averages for the 2nd group of samples ($v = 0.3$ m/s, $q = 1.45$).

It can be observed that the average difference between the measured and predicted wear values during the experiment is not more than 5.4 %. By the end of the experiment, the similarity between the predicted and measured wear values calculated is 99 %.

4.5. Conclusions

1. The following conclusions can be drawn from the analysis of the analytically calculated and experimentally obtained wear values for the sliding friction pair steel (102Cr6) – bronze (CW456K):
   - at $\boldsymbol{v = 0.7}$ m/s, $\boldsymbol{q = 0.58}$ MPa, the agreement between the analytically calculated and experimentally measured wear values at the end of the experiment is not less than 94.4 %;
   - at $\boldsymbol{v = 0.45}$ m/s and $\boldsymbol{q = 0.87}$ MPa, the agreement between the analytically calculated and experimentally measured wear values at the end of the experiment is not less than 85 %;
   - at $\boldsymbol{v = 0.3}$ m/s and $\boldsymbol{q = 1.45}$ MPa, the agreement between the analytically calculated and experimentally measured wear values at the end of the experiment is not less than 96.2 %.

2. The analysis of the obtained values of the surface texture (3D) parameters for the 1st group of samples after running-in stage shows that they increase with decreasing sliding speed and increasing load:
   - *Sa* for the third option (highest load and lowest speed) increases by 61 % compared to the first option and by 59 % compared to the second option;
   - RSm_1 increases by 53 % in option 3 compared to option 1 and by 6 % compared to option 2;
   - RSm_2^a increases by 16.4 % in the third option compared to the first option and by 20 % compared to the second option.

The effect of the parameters considered on wear is as follows. An increase in the *Sa* parameter leads to an increase in the wear values. This means that the higher the surface roughness of the friction surface, the weaker its resistance to deformation, resulting in greater wear. On the other hand, the step parameters RSm_1 and RSm_2^a have the opposite effect: the higher the step values, the higher the surface roughness of the friction surface, resulting in a more resistant surface to deformation. This, in turn, reduces wear.

1. The analysis of the wear values obtained for the sliding friction pair steel (102Cr6) – bronze (CW307G) – shows:
   - at $\boldsymbol{v = 07}$ m/s and $\boldsymbol{q = 058}$ MPa, the agreement between the analytically calculated and experimentally measured wear values at the end of the experiment is not less than 94.8 %;
   - at $\boldsymbol{v = 0.45}$ m/s and $\boldsymbol{q = 0.87}$ MPa, the agreement between the analytically calculated and experimentally measured wear values at the end of the experiment is not less than 95.8 %;
   - at $\boldsymbol{v = 0.3}$ m/s and $\boldsymbol{q = 1.45}$ MPa, the agreement between the analytically calculated and experimentally measured wear values at the end of the experiment is not less than 99.1 %.

2. For the 2nd group of samples a similar trend can be observed in the measurement of the surface texture (3D) parameters after running-in period, i.e., with increasing load and decreasing speed, the values of *Sa,* RSm_1 and RSm_2^a also increase:
   - *Sa* for the third option increases by 53 % compared to the first option and by 51 % compared to the second option;
   - RSm_1 increases by 66 % in option 3 compared to option 1 and by 51 % compared to option 2;
   - RSm_2^a increases by 65 % in option 3 compared to option 1 and by 62 % compared to option 2.

3. During the experimental studies, the samples of the1st group showed fluctuations in friction coefficient, which ranged up to 20 %. This made it difficult to determine the end of the running-in stage. That is why the surface texture parameters could also be exposed to cyclic variations with a wider range of values than in the normal

(stable) friction process. The analysis of the data suggests that these variations may have contributed to an increase in the difference between the theoretical and experimental linear wear values.

4. It is recommended to precisely determine the end of the running-in process during experiments to obtain wear calculation values as close as possible to the experimental data. This will result in a minimum range of numerical values of surface texture parameters (Sa, RSm_1, RSm_2^a) involved in the friction process after the running-in period and allow for a more accurate determination of wear by analytical calculation.
5. The proposed wear calculation model is valid for wear calculations in practical engineering tasks. Analytically calculated and experimental wear values at a given kinematic, applied load, surface texture (3D), and fatigue parameters show that the wear calculation Eq. (2.15) reliably obtains wear values. The difference between the experimental and analytically calculated wear values for all but one of the variants considered did not exceed the 5.6 % limit. The calculation of wear is simple and is saving time, financial, and technical resources needed for long-term wear experiments.
6. Further research is needed to analyse the wear calculation model in more detail and to correlate the parameters in Eq. (2.15) in the wear process for other materials at different loads, speeds, and surface texture (3D) parameters.

5. METHODOLOGY FOR PREDICTING LINEAR WEAR OF SLIDING FRICTION PAIR

The methodology developed for predicting the wear of a sliding friction pair is designed to determine the linear wear and/or linear wear rate of metallic surfaces in sliding friction pairs. This can be done without the need for expensive experiments, which can be time-consuming and inconvenient. This methodology can be used in both research and practical engineering calculations for the design of mechanisms whose components are subjected to sliding friction motion and wear. By applying this methodology, one can predict the service life of the friction pair during the design process by selecting appropriate materials and technological operations for the machining of component surfaces.

The methodology for predicting the wear of a sliding friction pair involves the following sequential steps (Fig. 5.1).

1. The constructive-kinematic parameters of the friction pair must be determined:
   1.1. Load q [MPa].
   1.2. The sliding speed $\boldsymbol{v}$ [m/s].
   1.3. The friction pair's sliding time $\boldsymbol{t}$ [s].
2. Using technical literature, determine the fatigue and physico-mechanical parameters of the material of the friction pair wearing part:
   2.1. Number of cycles to material's destruction $\boldsymbol{N_0}$.
   2.2. The degree of fatigue curve equation – $\boldsymbol{m}$.
   2.3. The limit of the material's durability in tension-compression – $\boldsymbol{\sigma_0}$ [MPa]:

$$\sigma_0 \approx 0.5 \cdot \sigma_{st}, \tag{5.1}$$

where σ_{st} is the ultimate strength of the material in MPa.

   2.4. Modulus of elasticity $\boldsymbol{E}$ [MPa].
3. Surface texture (3D) parameters* shall be determined according to EN ISO 25178:
   3.1. Arithmetic mean deviation from the midplane – $\boldsymbol{Sa}$.
   3.2. Step for worn workpiece surface perpendicular to machining direction – $\boldsymbol{RSm_1}$.
   3.3. The average surface roughness step of the surface contributing to the abrasion of the other surface – RSm_2^a.
   3.4. Coefficient of anisotropy of the surface of the worn part $\boldsymbol{Str}$.
4. Coefficient for elastic contact $\boldsymbol{k_q}$ should be chosen based on *Str*.
5. Calculate the linear wear at the given parameters using the wear calculation Eq. (2.15).
6. **The calculation of the linear rate of wear is carried out according to Eq. (2.16).
7. **The lifetime of a pair of sliding frictions is determined by the following relationship:

$$T = \frac{U_l}{V_{U_l}}, \tag{5.2}$$

where U_l is the linear wear and V_{U_l} is the linear rate of wear.

*The measurement of surface texture (3D) parameters for friction surfaces in point 3 of the Methodology is recommended after the end of the running-in period, when the major asperities of the friction parts have separated during the running-in process and the actual contact area has stabilised.

**Calculation of the wear rate and service life of a sliding friction pair is made as necessary.

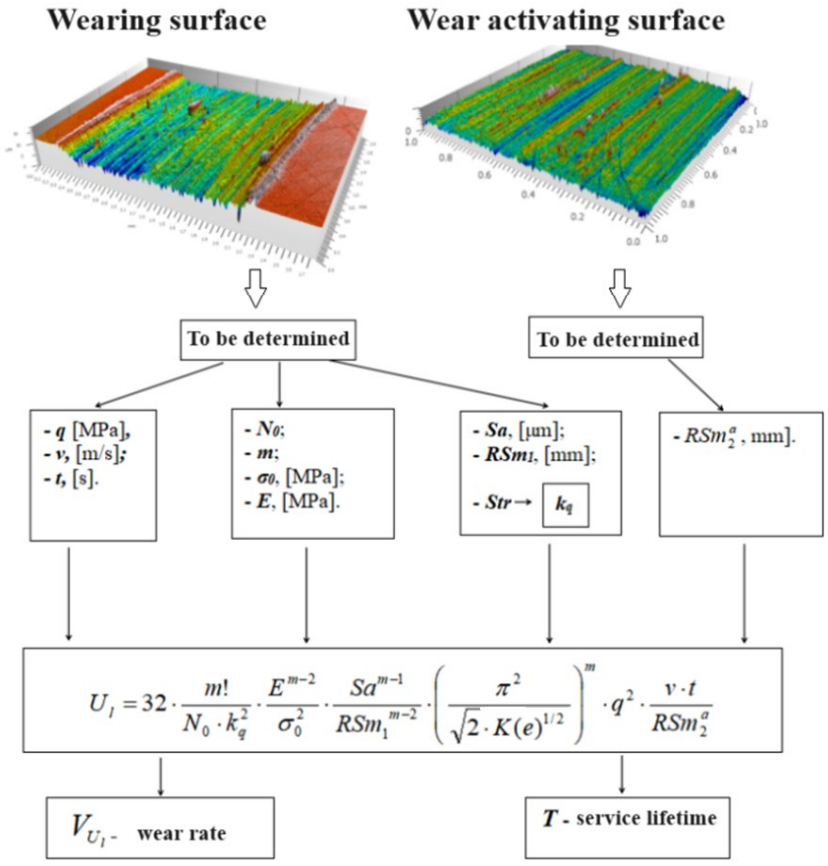

Fig. 5.1. Implementation algorithm for predicting linear wear of a sliding friction pair.

MAIN RESULTS AND CONCLUSIONS OF THE STUDY

Currently, there is no one universally accepted method for calculating wear. Most studies still rely on Archard's classical equation for analytical wear calculation, while some use Pronikov's or Kragelsky's models, which often involve values determined through long-term experiments, rather than analytical calculation. The roughness parameters used to describe surface micro-topography in these models are not standardized. The wear calculation model of Rudzitis et al. is considered to be more reliable for calculating friction surfaces, but it uses 2D roughness profile parameters that do not provide a complete picture of the actual microtopography of the surface. Recent studies have shown that 3D surface texture parameters provide a more complete and accurate description of the surface, which is critical for calculating frictional surface wear.

Therefore, in order to confirm the hypothesis of the Doctoral Thesis and to achieve the aim, the tasks of the Doctoral Thesis were fulfilled and the following **results** were achieved:

1. A new model of surface contact between friction parts based on normal random field theory has been synthesised. The model uses the surface texture (3D) parameters: a height parameter (*Sa*) and two surface roughness step parameters (RSm_1 and RSm_2) according to EN ISO 25178 to describe the friction surface. These three parameters provide a complete micro-topographic description of the friction surface for the calculation of friction wear.
2. A wear calculation model has been synthesised for a sliding friction pair on metallic surfaces using the experimental-theoretical calculation principle. The new wear calculation model is based on the new contact model for friction surfaces. The synthesised wear calculation model enables the analytical determination of the wear value as well as the analysis and optimisation of the parameters influencing the wear in the mechanism design process.
3. A new methodology for friction pair's lifetime calculations based on material's fatigue theory in friction and wear, including standardised parameter determination (including surface texture (3D) parameters), has been developed.
4. A research machine has been designed and built to investigate friction and wear processes. The machine was used to conduct preliminary research on the accuracy of wear values obtained from analytical calculations and experimental studies during the first phase.
5. Experimental validation of the new friction surface wear calculation model (the second phase of experimental studies) was carried out, showing close agreement between the calculated and experimentally determined wear values, which in most cases was not less than 94 %.
6. The experimental and analytical results analysis has indicated that there is a need for additional research on the impact of parameters that are not currently included in the wear calculation equation, and it is also important to investigate the correlation between the parameters that are already included.
7. The theoretical-experimental calculation method was applied in practice in project No. 1/22.05.2013-3 of Naco Ltd.

8. The calculation methodology of wear was validated in the mechanical engineering and metalworking industry by posting the methodology on the website of the Association of Mechanical Engineering and Metalworking (MASOC members' section).
9. Overall, it can be concluded that the research hypothesis of the PhD thesis "*The introduction of surface texture (3D) parameters, as well as the refinement of individual material fatigue parameter's values in the sliding friction pair wear calculation, will increase the accuracy of the calculation by synthesising a new mathematical model for the wear calculation and developing a methodology for predicting the lifetime of the friction pair.*" has been confirmed.

REFERENCES

1. Wujiao Xu, Wuhua Li, Yusong Wang. *Experimental and theoretical analysis of wear mechanism in hot-forging die and optimal design of die geometry*, Volume 318, Issues 1–2, 15 October 2014, pp. 78–88. DOI: https://doi.org/10.1016/j.wear.2014.06.021.
2. Adrian A. Schmidt, Timo Schmidt, Oliver Grabherr, Dirk Bartel. *Transient wear simulation based on three-dimensional finite element analysis for a dry running tilted shaft-bushing bearing*, Volumes 408–409, 15 August 2018, pp. 171–179. DOI: https://doi.org/10.1016/j.wear.2018.05.008.
3. S. Reichert, B. Lorentz, S. Heldmaier, A. Albers. *Wear simulation in non-lubricated and mixed lubricated contacts taking into account the microscale roughness*, Volume 100, August 2016, pp. 272–279. DOI: https://doi.org/10.1016/j.triboint.2016.02.009.
4. Wenjun Gong, Yunxia Chen, Mengwei Li, Rui Kang. *Coupling fractal model for adhesive and three-body abrasive wear of AISI 1045 carbon steel spool valves*, Volumes 418–419, 15 January 2019, pp. 75–85. DOI: https://doi.org/10.1016/j.wear.2018.10.019.
5. Wan-Gi Cha, Tobias Hammer, Florian Gutknecht, Roland Golle, A. Erman Tekkaya, Wolfram Volk. *Adaptive wear model for shear-cutting simulation with open cutting line*, Volumes 386–387, 15 September 2017, pp. 17–28. DOI: https://doi.org/10.1016/j.wear.2017.05.019.
6. Gao Deli, Sun Lianzhong and Lian Jihong. *Prediction of casing wear in extended-reach drilling*, Pet. Sci. (2010)7:494-501 DOI: 10.1007/s12182-001-0098-6.
7. José A. Brandão, Ramiro Martins, Jorge H. O. Seabra, Manuel J. D. Castro. *Calculation of gear tooth flank surface wear during an FZG micropitting test*, Volume 311, Issues 1–2, 15 March 2014, pp. 31–39. DOI: https://doi.org/10.1016/j.wear.2013.12.025.
8. Fei Lyu, Junhui Zhang, Guangming Sun, Bing Xu, Min Pan, Xiaochen Huang, Haogong Xu. *Research on wear prediction of piston/cylinder pair in axial piston pumps*, Volumes 456–457, 15 September 2020, 203338. DOI: https://doi.org/10.1016/j.wear.2020.203338https://doi.org/10.1016/j.wear.2020.203338.
9. Li Zhang, Hongli Gao, Dawei Dong, Guoqiang Fu and Qi Liu. *Wear Calculation-Based Degradation Analysis and Modeling for Remaining Useful Life Prediction of Ball Screw*, Volume 2018, Article ID 2969854, 18 pages. DOI: https://doi.org/10.1155/2018/2969854.
10. Kurt Frischmuth, Dirk Langemann. *Numerical calculation of wear in mechanical systems*, Volume 81, Issue 12, August 2011, pp. 2688–2701. DOI: https://doi.org/10.1016/j.matcom.2011.05.011.
11. Heinz Kloss, Rolf Wasche. *Analytical approach for wear prediction of metallic and ceramic materials in tribological applications*, Volume 266, Issues 3–4, 5 February 2009, pp. 476–481. DOI: https://doi.org/10.1016/j.wear.2008.04.034.
12. Jonaki Mukherjee, Sujan Ghosh, Arnab Ghosh, Ashok Ranjan, Arvind K. Saxena, Probal K. Das, Rajat Banerjee. *Enhanced nano-mechanical and wear properties of polycarbosilane derived SiC coating on silicon*, Volume 325, 15 January 2015, pp. 39–44. DOI: https://doi.org/10.1016/j.apsusc.2014.11.086.
13. Shirin Dehgahi, Rasool Amini, Morteza Alizadeh. *Corrosion, passivation and wear behaviors of electrodeposited Ni-Al2O3-SiC nano-composite coatings*, Volume 304, 25 October 2016, pp. 502–511. DOI: https://doi.org/10.1016/j.surfcoat.2016.07.007.
14. Lin Ding, Shengsun Hu. *Effect of nano-CeO2 on microstructure and wear resistance of Co-based coatings,* Volume 276, 25 August 2015, pp. 565–572. DOI: https://doi.org/10.1016/j.surfcoat.2015.06.014.
15. Pengbo Mi, Hongjian Zhao, Teng Wang, Fuxing Ye. *Sliding wear behavior of HVOF sprayed WC-(nano-WC-Co) coating at elevated temperatures*, Volume 206, 15 February 2018, pp. 1–6. DOI: https://doi.org/10.1016/j.matchemphys.2017.09.066.
16. Arash Yazdani, Taghi Isfahani. *Hardness, wear resistance and bonding strength of nano structured functionally graded Ni-Al2O3 composite coatings fabricated by ball milling*

method, Volume 29, Issue 5, May 2018, pp. 1306–1316. DOI: https://doi.org/10.1016/j.apt.2018.02.025.

17. J. C. Walker, S. R. Saranu, A. H. Kean, R. J. K. Wood. *Fe nano-particle coatings for high temperature wear resistance.* Wear, Volume 271, Issues 9–10, 29 July 2011, pp. 2067–2079. DOI: https://doi.org/10.1016/j.wear.2011.01.056https://doi.org/10.1016/j.wear.2011.01.056.
18. Xu Bin-shi, Wang Hai-dou, Dong Shi-yun, Jiang Bin. *Fretting wear-resistance of Ni-base electro-brush plating coating reinforced by nano-alumina grains,* Materials Letters 60 (2006) 710–713. DOI: 10.1016/j.matlet.2005.10.021.
19. Wenfang Cui, Gaowu Qin, Jingzhu Duan, Huan Wang. *A graded nano-TiN coating on biomedical Ti alloy: Low friction coefficient, good bonding and biocompatibility*, Volume 71, 1 February 2017, pp. 520–528. DOI: https://doi.org/10.1016/j.msec.2016.10.033.
20. Sajjad Ghasemi, Ali Shanaghi, Paul K. Chu. *Nano mechanical and wear properties of multi-layer Ti/TiN coatings deposited on Al 7075 by high-vacuum magnetron sputtering*, Volume 638, 30 September 2017, pp. 96–104. DOI: https://doi.org/10.1016/j.tsf.2017.07.049.
21. S. M. Lari Baghal, M. Heydarzadeh Sohi, A. Amadeh. *A functionally gradient nano-Ni-Co/SiC composite coating on aluminium and its tribological properties*, Volume 206, Issues 19–20, 25 May 2012, pp. 4032–4039. DOI: https://doi.org/10.1016/j.surfcoat.2012.03.084.
22. Hadi NasiriVatan, Reza Ebrahimi-Kahrizsangi, Masoud Kasiri Asgarani. *Tribological performance of PEO-WC nanocomposite coating on Mg Alloys deposited by Plasma Electrolytic Oxidation*, Volume 98, June 2016, pp. 253–260. DOI: https://doi.org/10.1016/j.triboint.2016.02.029.
23. Alexey A. Vereschaka, Sergey N. Grigoriev, Nikolay N. Sitnikov, Gaik V. Oganyan, Andre Batako. *Working efficiency of cutting tools with multilayer nano-structured Ti-TiCN-(Ti,Al)CN and Ti-TiCN-(Ti, Al, Cr)CN coatings: Analysis of cutting properties, wear mechanism and diffusion processes*, Volume 332, 25 December 2017, pp. 198–213. DOI: https://doi.org/10.1016/j.surfcoat.2017.10.027.
24. Praveenkumar Kiranagi, V. R. Kabadi. *Realistic Approach to Pin-on-Disc Wear Testing Measurement*, IJAPIE-SI-IDCM 610 (2017) 47-53 ISSN: 2455-8419.
25. Mohanad Bahshwan, Connor W. Myant, Tom Reddyhoff, Minh-Son Pham. *The role of microstructure on wear mechanisms and anisotropy of additively manufactured 316L stainless steel in dry sliding*, Volume 196, November 2020, 109076. DOI: https://doi.org/10.1016/j.matdes.2020.109076.
26. Iyas Khader, Dominik Kürten, Andreas Kailer. *A study on the wear of silicon nitride in rolling-sliding contact*, Volume 296, Issues 1–2, 30 August 2012, pp. 630–637. DOI: https://doi.org/10.1016/j.wear.2012.08.010.
27. B. Dirks, R. Enblom. *Prediction model for wheel profile wear and rolling contact fatigue*, Volume 271, Issues 1–2, 18 May 2011, pp. 210–217. DOI: https://doi.org/10.1016/j.wear.2010.10.028.
28. Yuanpei Chen, Fanming Meng. *Numerical study on wear evolution and mechanical behaviour of steel wires based on semi-analytical method*, Volume 148, November 2018, pp. 684–697. DOI: https://doi.org/10.1016/j.ijmecsci.2018.09.030.
29. Robert Tandler, Niels Bohn, Ulrich Gabbert, Elmar Woschke. *Analytical wear model and its application for the wear simulation in automotive bush chain drive systems,* Volumes 446–447, 15 April 2020, DOI: https://doi.org/10.1016/j.wear.2020.203193.
30. Weijun Tao, Yang Zhong, Hutian Feng, Yulin Wang. Model for wear prediction of roller linear guides, Volume 305, Issues 1–2, 30 July 2013, pp. 260–266. DOI: https://doi.org/10.1016/j.wear.2013.01.047.
31. V.L. Popov, R. Pohrt. Adhesive wear and particle emission: Numerical approach based on asperity-free formulation of Rabinowicz criterion, Friction 6(3): 260–273 (2018), ISSN 2223-7690 DOI: https://doi.org/10.1007/s40544-018-0236-4.

32. Valentin Popov. *GENERALIZED ARCHARD LAW OF WEAR BASED ON RABINOWICZ CRITERION OF WEAR PARTICLE FORMATION,* Series: Mechanical Engineering Vol. 17, No1, 2019, pp. 39–45. DOI: https://doi.org/10.22190/FUME190112007P.
33. Tongyan Yue and Magd Abdel Wahab. *A Review on Fretting Wear Mechanisms, Models and Numerical Analyses,* CMC, vol. 59, no. 2, pp. 405–432, 2019. DOI: 10.32604/cmc.2019.04253.
34. Yanfei Liu, Tomasz W. Liskiewicz, Ben D. Beake. Dynamic changes of mechanical properties induced by friction in the Archard wear model, Volumes 428–429, 15 June 2019, pp. 366–375. DOI: https://doi.org/10.1016/j.wear.2019.04.004.
35. Oskars Linins, Juris Krizbergs, Irina Boiko. Wear Estimation using 3D Surface Roughness Parameters, Vol. 527 (2013) pp. 167–172. DOI: 10.4028/www.scientific.net/KEM.527.167.
36. Natalija Bulaha, Janis Rudzitis. *ANALYSIS OF MODEL AND ANISOTROPY OF SURFACE WITH IRREGULAR ROUGHNESS*, Jelgava, 24–26.05.2017. DOI: 10.22616/ERDev2017.16.N241.
37. Natalia Bulaha. *CALCULATIONS OF SURFACE ROUGHNESS 3D PARAMETERS FOR SURFACES WITH IRREGULAR ROUGHNESS*, Jelgava, 23–25.05.2018. DOI: 10.22616/ERDev2018.17.N256 .
38. Ernests Jansons, Janis Lungevics, Uldis Kanders, Armands Leitans, Guna Civcisa, Oskars Linins, Karlis Kundzins and Irina Boiko. *Tribological and Mechanical Properties of the Nanostructured Superlattice Coatings with Respect to Surface Texture*. Lubricants 2022,10, 285. DOI: https://doi.org/10.3390/lubricants10110285.
39. A. Kromanis, J. Krizbergs. *3D SURFACE ROUGHNESS PREDICTION TECHNIQUE IN ENDMILLING USING REGRESSION ANALYSIS* 6th International DAAAM Baltic Conference INDUSTRIAL ENGINEERING, 2008, Tallinn.
40. A. Logins, T. Torims. The Influence of High-Speed Milling Strategies on 3D Surface Roughness Parameters, Volume 100, 2015, pp. 1253–1261. DOI: https://doi.org/10.1016/j.proeng.2015.01.491.
41. Kumermanis M. Investigations of 3D roughness parameters of irregular surfaces of rigid bodies. Riga, RTU Publishing House, 2011. p. 119. ISBN 2-86272-389-4.
42. Lorena Deleanu, Constantin Georgescu, Cornel Suciu. *A COMPARISON BETWEEN 2D AND 3D SURFACE PARAMETERS FOR EVALUATING THE QUALITY OF SURFACES,* 2012, ISSN 1221- 4566.
43. Jibin Boban, Afzaal Ahmed. *Improving the surface integrity and mechanical properties of additive manufactured stainless-steel components by wire electrical discharge polishing,* Volume 291, May 2021, 117013. DOI: httpshttps://doi.org/10.1016/j.jmatprotec.2020.117013doi.org/10.1016/j.jmatprotec.2020.117013.
44. M. Rezayat, M. Karamimoghadam, M. Moradi, G. Casalino, J. J. Roa Rovira and A. Mateo. *Overview of Surface Modification Strategies for Improving the Properties of Metastable Austenitic Stainless Steels,* Metals 2023, 13(7), 1268. DOI: https://doi.org/10.3390/met13071268.
45. G. Springis, J. Rudzitis, J.Lungevics, K. Berzins. Wear Calculation Approach for Sliding-Friction Pairs. *Journal of Physics*. Series 843 (2017) 012072. 2017, pp. 1-8. ISSN 1742-6588.DOIdoi: 10.1088/1742-6596/843/1/012072.
46. G. Springis, J. Rudzitis, A. Avisane, A. Leitans. Wear Calculation for Sliding Friction Pairs, Latvian Journal of Physics and Technical Sciences, Vol. 2, 2014, pp. 41–54, DOI: 10.2478/lpts-2014-0012.
47. Oskars Linins, Armands Leitans, Guntis Springis, Janis Rudzitis. *Determining the Number of Peaks of Rough Surfaces Necessary for Wear Calculation*, Trans Tech Publications, Switzerland, Key Engineering Materials, Vol. 604, 2014, pp. 59–62, DOI:10.4028.

48. J. Rudzitis. *Contact Mechanics of Surfaces Part 1*. Surface roughness profile parameters. Riga, Riga Technical University, 2007. 193 p. ISBN 978-9984-9964-1-7.
49. J. Rudzitis. *Contact Mechanics of Surfaces Part 2*. Microtopography of surface roughness profile. Riga, Riga Technical University, 2007. 217 p. ISBN 978-9984-9964-2-4.
50. J. Rudzitis. *Surface contact mechanics, Part 3. Calculations of sliding surface abrasion*. Riga, RTU Publishing House, 2007. p. 80. ISBN 9984-32-863-5.
51. G. Konrads. *Wear of sliding surfaces of machine parts.* Riga, RTU Publishing House, 2006. p. 80. ISBN 9984-32-863-5.
52. A. S. Pronikov. Parametric Reliability of Machines, Moscow: N. E. Bauman Moscow State Technical University Publishing House, 2002. 560 p. ISBN 5-7038-1996-2.
53. I. V. Kragelsky, M. N. Dobychin, V. S. Combalov. Fundamentals of Friction and Wear Calculations. Moscow, Mashinostroenie, 1977. 526 p.
54. I. V. Kragelsky and V. V. Alisina. Fundamentals Friction, Wear and Lubrication. Moscow, Mashinostroenie 1978. 400 p. (in Russian)
55. V. M. Musalimov, A. A. Sizova, E. K. Ivanov, N. A. Krylov, A. L. Tkachev. Osnovy Triboniki, textbook, St. Petersburg, 2009, 77 p. (in Russian)
56. D. N. Garkunov. Tribotechnics wear and tear. Textbook Moscow: Moscow State Agricultural University, 2001. 616 p. ISBN 5-94327-004-3. (in Russian)
57. I. Kragelsky, V. Alisin, Tribology – Lubrication, Friction and Wear, Mir publishers, Moscow, 2001.
58. Student E. *Calculation of sliding friction surface wear*. Riga, 1996. 135 p.
59. N. Bulaha, J. Rudzitis, J. Lungevics, O. Linins, K. Berzins. *Analysis and calculation of spacing parameters of anisotropic 3D surface roughness*. Latvian journal of physics and technical sciences, vol. 54, 2017.

Guntis Spriņģis was born in 1982 in Daugavpils. He obtained a Bachelor's degree and engineering qualification in Automobile Transport (2009) and an Academic Master's degree in Mechanical Engineering (2011) from Riga Technical University (RTU).
He has worked at Auteko & Tüv Latvija Ltd as a technical inspector of vehicles. Since 2009, he has been a laboratory assistant at Daugavpils Affiliation of RTU. Currently, he is a lecturer in mechanical engineering and mechanics (engineering technology) at the Daugavpils Study and Science Centre of RTU. He teaches several courses. His research interests include friction and wear processes and analysis and determination of their influencing parameters.